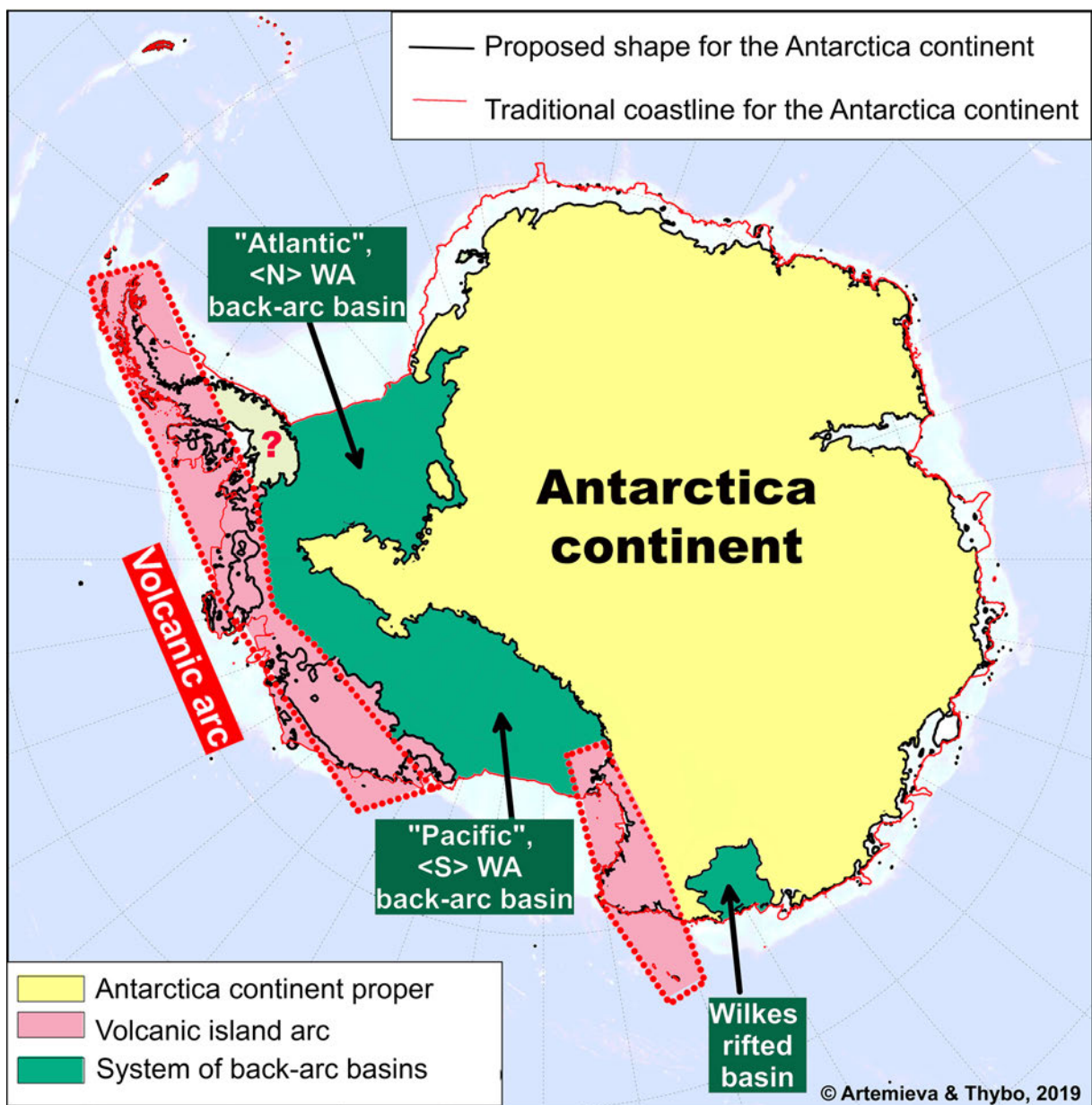


New map for the Antarctica continent



<https://doi.org/10.1016/j.earscirev.2020.103106>
Received 17 August 2019; Received in revised form <https://doi.org/10.1016/j.earscirev.2020.103106>

3
4 **Continent size revisited: Geophysical evidence for West Antarctica as a**
5 **back-arc system**
6

7 1
8
9 2 IRINA M. ARTEMIEVA (1,2) AND HANS THYBO (1,3,4)

10 3 (1) State Key Laboratory of Geological Processes and Mineral Resources, School of Earth Sciences,
11 4 China University of Geosciences, Wuhan, China

12 5 (2) Department of Geophysics, Stanford University, CA, USA

13 6 (3) Eurasia Institute of Earth Sciences, Istanbul Technical University, Turkey

14 7 (4) Center for Earth Evolution and Dynamics (CEED), University of Oslo, Norway
15
16

17 8 **Abstract**

19
20 9 Antarctica has traditionally been considered continental inside the coastline of ice and
21 10 bedrock since *Press and Dewart (1959)*. Sixty years later, we reconsider the conventional
22 11 extent of this sixth continent. Geochemical observations show that subduction was active along
23 12 the whole western coast of West Antarctica until the mid-Cretaceous after which it gradually
24 13 ceased towards the tip of the Antarctic Peninsula. We propose that the entire West Antarctica
25 14 formed as a back-arc basin system flanked by a volcanic arc, similar to e.g. the Japan Sea,
26 15 instead of a continental rift system as conventionally interpreted. Globally, the fundamental
27 16 difference between oceanic and continental lithosphere is reflected in hypsometry, largely
28 17 controlled by lithosphere buoyancy. The equivalent hypsometry in West Antarctica (-580 ± 335
29 18 m on average, extending down to -1.6 km) is much deeper than in any continent, but
30 19 corresponds to back-arc basins and oceans proper. This first order observation questions the
31 20 conventional interpretation of West Antarctica as continental, since even continental shelves
32 21 do not extend deeper than -200 m in equivalent hypsometry.

33
34
35
36 22 We present a suite of geophysical observations that supports our geodynamic
37 23 interpretation: a linear belt of seismicity sub-parallel to the volcanic arc along the Pacific
38 24 margin of West Antarctica; a pattern of free air gravity anomalies typical of subduction
39 25 systems; and extremely thin crystalline crust typical of back-arc basins. We calculate residual
40 26 mantle gravity anomalies and demonstrate that they require the presence of (1) a thick
41 27 sedimentary sequence of up to ca. 50% of the total crustal thickness or (2) extremely low
42 28 density mantle below the deep basins of West Antarctica and, possibly, the Wilkes Basin in
43 29 East Antarctica. Case (2) requires the presence of anomalously hot mantle below the entire
44 30 West Antarctica with a size much larger than around continental rifts. We propose, by analogy
45 31 with back-arc basins in the Western Pacific, the existence of rotated back-arc basins caused by
46 32 differential slab roll-back during subduction of the Phoenix plate under the West Antarctica
47 33 margin. Our finding reduces the continental lithosphere in Antarctica to 2/3 of its traditional
48 34 area. It has significant implications for global models of lithosphere-mantle dynamics and
49 35 models of the ice sheet evolution.

50
51
52
53 36 **Keywords:** Continental crust, lithosphere, upper mantle, paleosubduction, back-arc extension

37 1. General tectonic framework

38 The geology of Antarctica is largely unknown due to the cover by the up-to 3.5 km thick
39 ice sheet (Fig. 1) (Tingey, 1991; Fretwell et al., 2013), with only sparse outcrops of bedrock
40 (Fig. 2b). The continent traditionally includes 3 major tectonic units (Fig. 2a): the stable cratonic
41 East Antarctica which is separated by the Transantarctic Mountain belt (a 2.1-1.8 Ga orogen
42 (Zhao et al., 2002) reactivated in Cambrian during the time of the Pan-African orogenic event)
43 from the younger, extended lithosphere of West Antarctica. Since the focus of this study is on
44 West Antarctica, we omit details on tectonic evolution of the East Antarctica craton and the
45 Transantarctic Mountains (see e.g. Dalziel, 1992; Fitzsimons, 2000; Ferraccioli et al., 2011).

46 West Antarctica consists of several tectonic terranes that acted individually during the
47 break-up of Gondwana (Storey et al., 1988; Storey & Alabaster, 1991). The only dated
48 Precambrian rocks (of Grenvillian age) in West Antarctica are from the Haag Nunataks at the
49 Antarctic Peninsula end of the Ellsworth-Whitmore mountains (Wareham et al., 1998), which
50 form a topographic basement high across West Antarctica (Fig. 1a, 2ab). This basement high,
51 possibly also Precambrian in age (Dalziel and Elliot, 1982), separates two large, broad and
52 unusually deep depressions in equivalent topography, to which we refer as the “southern”
53 (<S>) and “northern” (<N>) West Antarctica basins (Fig. 3), although strictly speaking such
54 geographical terms are meaningless around the pole.

- 55 • The southern domain, that extends from the Ross Ice Shelf to the Antarctic Peninsula and
56 includes Marie Byrd and Ellsworth Land, has long been recognized as one of the world’s
57 largest crustal extensional areas with a size of ca. 3000 km x 1000 km (Stock and Molnar,
58 1987; Bradshaw, 1989; Lawver et al., 1991; Behrendt, 1991; 2013; Cande et al., 2000;
59 Harley, 2003; Siddoway, 2008; Ramirez et al., 2016).
- 60 • The northern domain, which includes the Ronne Ice Shelf, has been interpreted as formed
61 by extension during the Mesozoic breakup of Gondwana and possibly caused by rotations
62 during the opening of the Weddell Sea between South America and Antarctica at ca. 165-
63 130 Ma (Behrendt, 1999; König and Jokat, 2006) (Fig. 3a).

64 Geological and geophysical studies indicate that the crust (possibly the entire lithosphere)
65 of West Antarctica has been subject to a significant extension and magmatism (Fig. 3) since
66 late Paleozoic, although the timing may be controversial (Stock and Molnar, 1987; Bradshaw,
67 1989; Cande et al., 2000; Granot et al., 2010). Geodynamic mechanisms of the extension are
68 also controversial, and plate reconfigurations during the Gondwana breakup possibly played
69 an important role in lithosphere extension (see section 3 below).

70 The southern domain is traditionally interpreted in the extensive literature as a continental
71 rift system. We next review various geodynamic hypotheses on the origin of lithosphere
72 extension in West Antarctica and propose an alternative explanation, based on the available
73 geophysical data and supported by our model for the upper mantle density structure.

2. Traditional geodynamic view on West Antarctica

2.1. West Antarctica Rift System

Traditionally <S> West Antarctica is perceived as the West Antarctica Rift System (LeMasurier and Rex, 1989; Behrendt et al., 1991; Hart et al., 1997; Behrendt, 1999; 2013; Cande et al., 2000; Ritzwoller et al., 2001; Harley, 2003; Siddoway et al., 2004; Huerta and Harry, 2007; Siddoway, 2008; Buseti et al., 2009; Granot et al., 2010; Bingham et al., 2012; Darniani et al., 2014; An et al., 2015ab; Davey et al., 2016; Ramirez et al., 2016; Jordan et al., 2017; Fei et al., 2018; Granot and Dymant, 2018; White-Gaynor et al., 2019). It is also often mentioned as “one of the largest active continental rift systems on Earth” (Cande et al., 2000), “comparable in area to the Basin and Range and the East African rift system” (Behrendt et al., 1991), and with geodynamic development similar to the East African rift and other continental analogues (LeMasurier and Rex, 1989; LeMasurier, 2008). The mountain ranges that extend from the Ellsworth-Whitmore mountains in the north to the Transantarctic Mountains in the south have been interpreted as rift shoulders (Behrendt, 1991; Fitzgerald, 1992; van Wijk et al., 2008), with the opposing poorly defined rift shoulder at coastal outcrops of Marie Byrd Land (Fig. 2a).

Geological and geophysical observations for interpreting <S> West Antarctica as a wide continental rift system include (1) crustal extension and crustal thinning, (2) intensive volcanism and (3) hot mantle. We briefly summarize these observations below.

2.1.1. Crustal extension

West Antarctica is recognized as a broad zone of episodic crustal extension from geological (Dalziel and Elliot, 1982; Cooper and Davey, 1985; Lawver and Gahagan, 1994; Fitzgerald and Baldwin, 1997; Salvini et al., 1997) and high-resolution geophysical mapping (Houtz and Davey, 1973; Cooper et al. 1995; Studinger et al., 2002). In particular, aeromagnetic surveys and seismic reflection profiles established the presence of two subparallel grabens under the Ross Ice Shelf, filled with 7-8 km and 14 km of sediments, correspondingly (cf. Behrendt et al., 1991). The presence of a thin crust in West Antarctica, recognized from early seismic and gravity surveys of 1960-80's, has been confirmed by recent seismic experiments (cf. Baranov and Morelli, 2013; Chaput et al., 2014; An et al., 2015), which show crustal thickness of 20-30 km in West Antarctica with an average value of ca. 20 km in the Ross Sea, ca. 25 km in Marie Byrd Land and ca. 34 km in Ellsworth Land (Fig. 4). These values are significantly lower than typical thickness of continental crust (Christensen and Mooney, 1995; Artemieva and Shulgin, 2019) and indicate strong crustal extension.

The estimated maximum crustal extension in <S> West Antarctica since late Cretaceous until present ranges from 250 km to 350 km (cf. Behrendt, 1999), with ca. 150 km of extension between 68 Ma and 46 Ma at the Ross Sea segment (Cande and Stock, 2004), ca. 180 km extension in its northwestern part between 43 Ma and 26 Ma (Cande et al., 2000), and another extensional episode at the Ross Sea at ca. 11 Ma (Granot and Dymant, 2018). Estimates of the

178
179
180
181 112 whole crust stretching factor for the Ross Subglacial Basin based on gravity modeling yield
182 113 extremely high values of $\beta \sim 3$ on average with local maximum of $\beta > 4$ (*Fei et al., 2018*), which
183 114 are not observed in any continental rift zones (*McKenzie, 1978; Thybo and Nielsen, 2009*).
184 115 These values are in contrast to $\beta \sim 2$ estimated for stretching of the entire lithosphere beneath
185 116 the West Antarctica Rift System (*Behrendt et al., 1991*). However, the latter may be strongly
186 117 underestimated in the absence of reliable models on the lithosphere structure in Antarctica in
187 118 1990ies. Since late Paleogene, extension slowed down and became restricted to the Ross
188 119 Subglacial Basin (*Huerta and Harry, 2007*), with no present-day extension resolved by GPS
189 119 measurements in West Antarctica (*Wilson et al., 2015*).
190
191

192 193 121 2.1.2. Meso-Cenozoic basaltic volcanism

194
195 122 Volcanic activity in West Antarctica began in the Mesozoic (**Fig. 3a**) and continued in
196 123 the Cenozoic along the coast of Marie Byrd Land, in the southern part of West Antarctica along
197 124 the Transantarctic mountains, and possibly in the interior of the West Antarctica domain
198 125 (*Behrendt et al., 1997; Fitzgerald and Baldwin, 1997; Hart et al., 1997; Siddoway, 2008*).
199 126 Since most volcanic rocks are under ice, the information on their volume and the age of
200 127 volcanism remains incomplete (*Blankenship et al., 1993*). An estimated volume of volcanic
201 128 rocks in West Antarctica interpreted from magnetic anomalies exceeds 1 mln km³ (*Behrendt*
202 129 *et al., 1994*).
203
204

205
206 130 Later Mesozoic volcanism has been explained by reorganization of lithosphere blocks
207 131 (*Dalziel and Elliot, 1982; Cande et al., 2000*), such as Late Cretaceous rifting and separation
208 132 of the New Zealand-Campbell Plateau from Antarctica (*Weaver et al., 1994; Luyendyk et al.,*
209 133 *1996*), or intraplate deformation and plate dynamics (*Rocchi et al., 2002, 2003, 2005*). The
210 134 geochemical composition of Cenozoic volcanic rocks is compatible with deep mantle melting
211 135 (*Behrendt, 1999; Worner, 1999; Rocchi et al., 2002*) and is similar to ocean plateau basalts
212 136 (*Hart et al., 1997*), suggesting a mantle plume as an alternative or additional mechanism to
213 137 lithosphere stretching (*Dalziel, 1992; Winberry and Anandkrishnan, 2004*). Late Cenozoic
214 138 volcanic activity is attributed to adiabatic mantle melting during continental rifting in West
215 139 Antarctica (*LeMasurier, 1990*). We further discuss the origin of Meso-Cenozoic volcanism in
216 140 **section 3**.
217
218
219

220 221 141 2.1.3. Hot mantle?

222
223 142 Overall, the resolution of regional seismic tomography models for Antarctica is limited
224 143 due to insufficient ray path coverage: although seismicity at the ring of mid-ocean ridges
225 144 around the Antarctic plate provides a good azimuthal coverage, the distribution of seismic
226 145 stations remains sparse. As a result, details of the upper mantle structure beneath West
227 146 Antarctica are controversial. Regional seismic tomography models show slow seismic
228 147 velocities in the upper mantle of West Antarctica, in contrast to a typical cold and thick cratonic
229 148 lithosphere of the East Antarctic craton (*Danesi and Morelli, 2001; Ritzwoller et al., 2001;*
230 149 *Sieminski et al., 2003; Morelli and Danesi, 2004; Hansen et al., 2014; An et al., 2015b*). All
231
232

237
238
239
240
241
242
243
244
245
246
247
248
249
250
251
252
253
254
255
256
257
258
259
260
261
262
263
264
265
266
267
268
269
270
271
272
273
274
275
276
277
278
279
280
281
282
283
284
285
286
287
288
289
290
291
292
293
294
295

150 geodynamic interpretations of slow seismic velocity anomalies favor lithosphere rifting in case
151 of shallow (above a 200 km depth) anomalies and a possible role of mantle plumes for deep-
152 seated velocity anomalies imaged beneath Marie Byrd Land (*Hansen et al., 2014; Lloyd et al.,*
153 *2015*) and the Ross Embayment (*Bannister et al., 2000; Danesi and Morelli, 2001*). Slow
154 seismic velocity anomalies are interpreted in terms of high upper mantle temperatures and thin
155 lithosphere in West Antarctica (*Shapiro and Ritzwoller, 2004; An et al., 2015a*) (Fig. 5a).

156 Flexural modeling also suggests a sharp transition across the Ross Embayment at the
157 Transantarctic Mountains with a thin (<100 km) elastic lithosphere beneath West Antarctica
158 and a 250 km thick lithosphere beneath the East Antarctic craton (*Stern and ten Brink, 1989*).
159 The same model assumes that at 100 km depth the upper mantle beneath the Ross Subglacial
160 Basin is ca. 600 °C hotter than beneath the craton (*ten Brink et al., 1997*), whereas a thermal
161 model suggests a temperature difference of ca. 300 °C between the Ross Subglacial Basin and
162 the East Antarctic craton at a 100 km depth (*Artemieva, 2006*).

163 A high resolution seismic transect across Marie Byrd Land and Byrd Subglacial Basin
164 reveal significant velocity heterogeneity of the West Antarctic upper mantle (*Lloyd et al.,*
165 *2015*). Relatively fast P- and S- velocities beneath the Ellsworth-Whitmore mountains and
166 most of the West Antarctic Rift System are interpreted to represent a possible Precambrian
167 lithosphere fragment, while slow velocity anomalies beneath a deep narrow subglacial basin
168 (the Bentley Subglacial Trench) and the central coast in Marie Byrd Land are interpreted as
169 consistent with a plume-related warm upper mantle (*Lloyd et al., 2015*).

170 One of the peculiar features imaged in a surface wave tomography model is a high
171 velocity anomaly in the upper mantle beneath the Antarctic Peninsula, which has been
172 interpreted as a slab associated with an Eocene subduction along the coast of the Antarctic
173 Peninsula, Marie Byrd Land, and Ellsworth Land (*An et al., 2015a*). Despite this observation,
174 no inference was made to explain the slow velocity anomaly beneath the whole of West
175 Antarctica by backarc spreading, which the authors conventionally interpreted as the West
176 Antarctic Rift System, and their comparison of the West Antarctica Pacific margin with the
177 active Pacific margin in Asia focuses on the thin crust and lithosphere in onshore China, but
178 not on back-arc spreading in the Japan Sea (*An et al., 2015a*).

179 In general, there is a significant controversy in mantle temperature anomalies constrained
180 by different seismic tomography models and magnetic methods, both in the amplitudes and the
181 locations. Targeted magnetotelluric profiling across the Byrd Subglacial Basin of central West
182 Antarctica did not image a strong conductivity anomaly as expected for active rift zones
183 (*Wannamaker et al., 1996*). In contrast, the presence of a hot upper mantle with a shallow Curie
184 depth beneath the Byrd Subglacial Basin is suggested from the analysis of airborne magnetic
185 data (*Martos et al., 2017*), although satellite magnetic data suggests that the strongest anomaly
186 is located beneath <N> West Antarctica, and not beneath <S> West Antarctica (*Fox Maule et*
187 *al., 2005*).

2.2. Alternative geodynamic models : Plumes and plates

Until present, West Antarctica is tagged in the literature as “West Antarctica Rift System”, and most interpretations maintain this geodynamic model (*LeMasurier and Rex, 1989; Behrendt et al., 1991; Hart et al., 1997; Behrendt, 1999; 2013; Cande et al., 2000; Ritzwoller et al., 2001; Harley, 2003; Siddoway et al., 2004; Huerta and Harry, 2007; Siddoway, 2008; Buseti et al., 2009; Eagles et al., 2009; Faure and Mensing, 2010; Granot et al., 2010; Jordan et al., 2010, 2013; Bingham et al., 2012; Darniani et al., 2014; An et al., 2015ab; Lloyd et al., 2015; Davey et al., 2016; Ramirez et al., 2016; Jordan et al., 2017; Fei et al., 2018*). Importantly, the geodynamic processes behind the continental rifting analogues are based on rifting in long linear zones of continental lithospheric plates (*Olsen, 1995*) due to either deep thermal anomalies (*Ritzwoller et al., 2001*) or far-field tectonic stresses (*Sengör and Burke, 1978*).

These extensional systems above sea level must have a different geodynamic origin than the West Antarctica basins, which are submerged deep below sea level and are neither localized linear zones of extension (*McKenzie, 1978*), as in continental rift zones, nor broad areas of homogeneous extension, as in the Basin and Range Province (*Wernicke, 1981*). Instead, they represent broad depressions with a superimposed series of basins at extremely deep equivalent hypsometry (corrected by compressing ice and water masses to the density 2.67 g/cm³ of near-surface rocks), on average 580 m below sea level (**Fig. 3a**) which is much deeper than observed anywhere else in continental rift zones or other tectonic provinces on continental lithosphere (**Fig. 6**). Although the existence of deep submerged basins in West Antarctica has been known for decades, they were traditionally explained by lithosphere stretching of continental lithosphere; a possible contribution of phase transition and thermal subsidence (*Podladchikov et al., 1994*) as an alternative or an additional mechanism was estimated to be too low to explain large subsidence of the West Antarctic Rift System (*Behrendt, 1999*).

A brief overview in **section 2.1** indicates that the original perception from the 70-90’ies on the West Antarctica as a wide zone of continental rifting has been challenged by several authors, who emphasized the role of other mechanisms in Mesozoic – early Cenozoic extension and volcanism of West Antarctica:

- the Gondwana plate reconfiguration, Gondwana breakup and late Cretaceous rifting of the New Zealand-Campbell Plateau from Marie Byrd Land (*Jankowski and Drewry, 1981; Dalziel and Elliot, 1982; Stock and Molnar, 1987; Bradshaw, 1989; Lawver et al., 1991; Weaver et al., 1994; Luyendyk, 1995; Luyendyk et al., 1996; Cande et al., 2000; Siddoway, 2008; Veevers, 2012*);
- mantle plumes and convective instabilities (*Behrendt et al., 1991; Dalziel, 1992; Storey, 1996; Hart et al., 1997; Rocci et al., 2002; Winberry and Anandkrishnan, 2004; Finn et al., 2005; Hansen et al., 2014; Lloyd et al., 2015; Seroussi et al., 2017; Ebbing et al., 2019*);
- intraplate deformation (*Rocchi et al., 2003, 2005*) and lithosphere flexure (*Stern and ten Brink, 1989; ten Brink et al., 1997*), also due to sediment (*Karner et al., 2005*) and magmatic loading (*Jordan et al., 2010; Karner et al., 2005; Trey et al., 1999*);

- 355
356
357
358 229 • possible dynamic topography associated with mantle flow and subduction (e.g. *Spasocevic*
359 230 *et al., 2010; Sutherland et al., 2010*).

360 231 Here we propose an alternative hypothesis, that the entire West Antarctica formed by
361 232 back-arc extension in Mesozoic subduction settings along the Panthalassic (paleo-Pacific)
362 233 margin. Although this mechanism is related to the Gondwana plate reconfiguration and back-
363 234 arc extension has been mentioned by several authors in relation to tectonics of West Antarctica,
364 235 the role of this process has been severely underestimated. We next present a brief overview for
365 236 West Antarctica tectonic models during the Gondwana breakup.

370 237 **3. Gondwana breakup and Panthalassic subduction**

372 238 The amalgamation of the pre-Gondwana cratons accreted continental fragments and arc
373 239 material to the Panthalassic (paleo-Pacific) margin of Gondwana in late Cambrian - Cretaceous.
374 240 An overview of West Antarctica's position in Gondwana can be found in the extensive
375 241 literature on the subject (e.g. *Dalziel and Elliot, 1982; Vaughan and Pankhurst, 2008; Boger,*
376 242 *2011; Veevers, 2012; Dalziel et al., 2013*). Here we mention only major tectonic events
377 243 important for further discussion of the Meso-Cenozoic extension in West Antarctica (**Fig. 7**),
378 244 and in particular refer to the studies where back-arc extension is mentioned in various context.

382 245 **3.1. Mid-Jurassic/early Cretaceous Gondwana breakup**

385 246 The breakup of Gondwana, which started in the mid-Jurassic, led to the opening of the
386 247 Weddell Sea between South America and Antarctica at ca. 165-130 Ma (*Behrendt, 1999; Konig*
387 248 *and Jokat, 2006*). Possible rotations of the Ellsworth-Whitmore mountains lithosphere block
388 249 in West Antarctica during the opening of the Weddell Sea (although questioned recently,
389 250 *Jordan et al., 2017*) may have been caused by slab rollback associated with subduction beneath
390 251 southern Africa at ca. 185-180 Ma (*Dalziel et al., 2013; Jordan et al., 2017*).

392 252 Early Paleozoic to early Mesozoic back-arc terrains identified in regional geological
393 253 observations in outcrops around the Ronne Ice Shelf (*Dalziel and Elliot, 1982; Millar and*
394 254 *Storey, 1995*) (**Fig. 2b**) predate the opening of the Weddell Sea. Pillow-basalt flows of late
395 255 Cambrian to early Ordovician age in the Pensacola mountains were interpreted as rift-related,
396 256 with a possibility of a back-arc basin development (*Millar and Storey, 1995; cited in Faure*
397 257 *and Mensing, 2010*). Based on sparse outcrop of locally exposed volcanic detritus in the
400 258 Ellsworth mountains (*Dalziel and Elliot, 1982*), there were early speculations about possible
401 259 existence of a late Early Permian back-arc basin along the Panthalassic margin with an
402 260 undefined areal extent (*Collinson et al., 1994*) (see **Fig. 2b** for locations).

3.2. Early-mid Cretaceous subduction at the Panthalassic (paleo-Pacific) margin

The early Cretaceous separation of Australia coincided broadly with the collisional events along the West Antarctica margin (*Boger, 2011*), which included the collision of the Amundsen and Ross provinces of Marie Byrd Land by 107 Ma (*Mukasa and Dalziel, 2000; Vaughan et al., 2002*). Marie Byrd Land, Thurston Island block, and the Antarctic Peninsula are interpreted as fore-arc and magmatic arc terranes associated with the Cretaceous subduction of the Phoenix plate at the Panthalassic margin of Gondwana (*Dalziel and Elliot, 1982; Mukasa and Dalziel, 2000; Boger, 2011*) (**Fig. 7**), which terminated at 110-105 Ma (*Bradshaw, 1989*). Note that paleo-reconstructions fail to match the coast lines of the Antarctica Peninsular and the Gondwana continents in the Gondwana reconstructions (*Dalziel and Elliot, 1992*), and therefore it has long been proposed that the Antarctic Peninsula can be a “Mesozoic accretionary belt” (*Dietz and Sproll, 1970*).

Subduction related, calc-alkaline magmatism has been observed in Marie Byrd Land from ca. 320 Ma (the oldest granodiorite rocks) until ca. 110 Ma (the age of the youngest I-type granites) (*Mukasa and Dalziel, 2000*). I-type granitoids (124-108 Ma) of central Marie Byrd Land (the Ruppert-Hobbs coast, **Fig. 2b**) are interpreted as typical subduction-related magmas (*Weaver et al., 1994*). These authors find evidence that subduction of the Phoenix Plate below Marie Byrd Land ceased gradually from <S> to <N> between 108 and 95 Ma (**Fig. 7**). Mafic rocks with ages of 110-95 Ma from central Marie Byrd Land (the Ruppert-Hobbs coast, **Fig. 2b**) have composition of continental flood-basalt affinity typical of rift magmatism in the presence of plume-head (*Weaver et al., 1992, 1994*). Slightly younger wide-spread A-type granitoids with age of 102-95 Ma from eastern Marie Byrd Land (Edward VII Peninsula on the Ross Sea margin, **Fig. 2b**) are interpreted as associated with intracontinental rifting that later led to the separation of the Zealandia block from West Antarctica (*Weaver et al., 1992, 1994*).

Later, with reference to the same interpretations (*Weaver et al., 1992; 1994*), back-arc extension has been mentioned as a possible source of the mid-Cretaceous alkaline plutonism in eastern Marie Byrd Land for a short period of 105-102 Ma (*Siddoway, 2008; Damiani et al., 2014*), although the overall regional evolution was explained traditionally - by continental break-up and intracontinental rifting in the presence of a postulated mantle plume (*Siddoway, 2008*). A speculation on a possible existence of a back-arc basin in Byrd Subglacial Basin and in the far-eastern sector of the Transantarctic Mountains has been later repeated without new evidence (e.g. *Faure and Mensing, 2010*) and with reference to a study, where Neogene extension in West Antarctica rifts was inferred from comparisons with the East African rift system and the entire region was interpreted as the West Antarctica Rift System (*LeMasurier, 2008*).

3.3. Mid-/late-Cretaceous extension

In mid-Cretaceous (ca. 100 Ma) the composition of igneous rocks in central Marie Byrd Land changed from subduction-related to rift-related, indicating the change in stress regime from transpressional to transtensional (*Weaver et al., 1994*). At this time, Australia separated from Antarctica with the first seafloor formed in-between by 96 Ma (*Veevers et al., 1991*); the Zealandia block (including the New Zealand-Campbell Plateau) rifted away from Antarctica with the formation of the first seafloor by ca. 83 Ma (*Weaver et al., 1994; Luyendyk et al., 1996; Larter et al., 2002*). This separation formed the western margin of Antarctica as it is seen today (*Boger, 2011*) (**Fig. 7**).

Thereafter subduction ceased sequentially along the West Antarctica margin (*Dalziel, 1992*). A capture of the subducted Phoenix plate by the Pacific plate was proposed as a mechanism for extension (*Luyendyk, 1995*) based on geochemical data on magmatic rocks and ocean floor magnetic anomalies. Further <N> along the Antarctic Peninsula, subduction also gradually ceased from <S> to <N> after 94 Ma, and today the only remaining subduction is presently active at the South Shetlands Trench at the northern tip of the Antarctic Peninsula (*Storey and Garrett, 1984; Barker, 1982*).

4. Continent revisited: Equivalent topography - a first order observation

We conclude that not a single publication argue for the back-arc origin of the entire West Antarctica, including both <S> (Ross and Byrd Subglacial Basins) and <N> (Ronne Ice Sheet) domains. Geological interpretations consider late Cretaceous-Cenozoic intracontinental extension, possibly in the presence of a mantle plume, as the major tectonic process in <S> West Antarctica, and mostly without even mentioning back-arc extension as a possible mechanism (*Finn et al., 2005; Ferraccioli et al., 2006; Eagles et al., 2009; Jordan et al., 2010, 2013; Bingham et al., 2012*). The Meso-Cenozoic evolution of the ice-covered Ronne Ice Sheet is not discussed in literature, possibly due to lack of geological data. We next present geophysical evidence in support of our hypothesis for a back-arc origin of the entire West Antarctica and propose a geodynamic model for its Meso-Cenozoic evolution.

Hypsometry on Earth is largely controlled by lithosphere buoyancy and dynamic processes related to plate tectonics and mantle convection. Its bimodal distribution reflects the existence of two principally different lithosphere types, oceanic and continental (**Fig. 6**). On continental lithosphere hypsometry globally ranges from high elevations in young mountain belts and stable regions with dynamic topography, to 300-500 m elevation in cratons, and down to -200 m of equivalent hypsometry on continental shelves.

East Antarctica and the Transantarctic Mountain belt have high equivalent hypsometry typical of continental landmass (+1050±650 m on average, up to +3.5 km, **Fig. 3**) and East Antarctica shows all characteristics of normal cratonic lithosphere, with a 38-55 km thick crust (*Baranov & Morelli, 2013; Feng et al., 2014; An et al., 2015b; Ramirez et al., 2016*) (**Fig. 4**),

532
533
534 336 high seismic velocities in the upper mantle (*Ritzwoller et al., 2001; An et al., 2015a*), and
535 337 thicker than 150-250 km lithosphere (*An et al., 2015a*) (**Fig. 5b**).

537 338 In contrast, West Antarctica is characterized by unusually deep equivalent hypsometry (-
538 339 580±335 m on average, down to -1.6 km) (**Figs. 3, 6**). Such deep bathymetry as in West
540 340 Antarctica is globally observed nowhere in continents, while oceans proper usually are much
541 341 deeper (4-6 km for bathymetry and ca. 2.5-3.5 km for equivalent hypsometry). This first order
542 342 observation shows that West Antarctica consists of neither continental nor oceanic lithosphere,
543 343 while such hypsometry is common in many back-arc basins flanked by a volcanic arc on the
544 344 ocean side (*Dickinson, 1978; Uyeda & Kanamori, 1979; Brooks et al., 1984; Waschbusch &*
545 345 *Beaumont, 1996*) (**Figs. 6, 8-10**).

549 346 **5. Continent revisited: Geophysical observations in support of** 550 551 347 **back-arc tectonics**

553 348 We present geophysical evidence that most of West Antarctica represents a Mesozoic to
554 349 Cenozoic back-arc system with two main basins separated by the Ellsworth-Whitmore
555 350 mountains, in contrast to conventional interpretations of West Antarctica as a continental rift
556 351 system. We recognize the following features typical of back-arc systems worldwide (*Wernicke,*
557 352 *1981*) (**Fig. 9**):

- 560 353 1) the presence of a volcanic arc along the Pacific margin of West Antarctica (**Fig. 3b, 8**),
- 561 354 2) the presence of a sub-parallel, linear belt of seismicity deepening towards the volcanic arc
562 355 (**Fig. 3b, 8**),
- 563 356 3) a linear pattern of free air gravity anomalies along the Pacific margin of West Antarctica
564 357 typical of subduction systems (**Fig. 11a**),
- 565 358 4) the presence of an extremely thin crystalline crust over broad basins of West Antarctica (**Fig.**
566 359 **4**) typical of back-arc basins, in contrast to typically linear belts of thin crust in continental
567 360 rift zones (*Olsen, 1995*),
- 568 361 5) the presence of a thin and hot lithosphere over broad basins of West Antarctica (**Fig. 5ab**).

570 362 We briefly review these features below and then support our interpretation by a new
571 363 density model of the West Antarctica lithosphere.

574 575 576 364 **5.1. Volcanism**

577
578 365 The West Antarctica basin system is flanked in the west by the (partly extinct) volcanic
579 366 arc along the Pacific-Antarctic paleosubduction zone (**Fig. 3b**), with volcanic age decreasing
580 367 <S-ward> (*Jordan et al., 2017*) (**Fig. 3a**) from Triassic-Cretaceous in the Antarctic Peninsula
581 368 (*Collinson et al., 1994; Riley & Leat, 1999; Vaughan & Storey, 2000; Harley, 2003*), to
582 369 Cretaceous arc-related granitoids (*Weaver et al., 1992; 1994; Mukasa & Dalziel, 2000*) and
583 370 recent volcanic activity (*Lemasurier & Rex, 1989; Hart et al., 1997*) in Marie Byrd Land, and
584 371 to the active volcanoes at the end of the Transantarctic Mountains at the Ross Sea (*Kyle &*

591
592
593 372 *Muncy, 1989*), although a few recently active volcanoes also exist at the tip of the Antarctic
594 373 Peninsula (*Larter & Barker, 1991*). This volcanic belt forms a narrow elongated zone with
595 374 positive equivalent topography between the Pacific Ocean and the West Antarctica basin
596 375 system (*Fig. 3b*).

600 376 **5.2. Seismicity**

602 377 We interpret a linear belt of shallow (<40 km and mostly crustal) magnitude 4.2-6.3
603 378 seismicity (*Fig. 3b, 8*), as well as aligned mantle earthquakes parallel to the volcanic arc, as
604 379 related to paleosubduction of the Phoenix plate below West Antarctica (*Fig. 3b*). We emphasize
605 380 that the seismicity does not reflect present day subduction (which ceased along the Marie Byrd
606 381 margin in late Cretaceous), but instead follows the weakness zones created during paleo-
607 382 subduction. The pattern of arc-related volcanism between a parallel belt of seismicity on the
608 383 ocean side and deep basins on the continental side is similar to the volcanic arcs in the
609 384 subduction systems of the NW Pacific Ocean which have back-arc basins (*Van Horne et al.,*
610 385 *2015*) (e.g. Japan and the Aleutians, *Fig. 8*).

616 386 **5.3. Gravity anomalies**

618 387 Subduction systems have a unique pattern of free air gravity anomalies across strike with
619 388 strong negative anomalies above trenches followed by weak positive anomalies towards the
620 389 volcanic arc (*Artemieva et al., 2016*). We observe a similar pattern of free air gravity anomalies
621 390 along the Pacific margin of West Antarctica with a linear belt of negative (-100-40 mGal)
622 391 anomalies as the gravity signal from the trench, which today has been isostatically readjusted
623 392 and filled with sediments, and a parallel narrow belt of positive (+10+70 mGal) free air
624 393 anomalies on the side of the volcanic arc (*Fig. 8a, 11a*). Seismicity is restricted to the belt of
625 394 negative free air anomalies and its ocean-ward vicinity (*Fig. 3b, 8b*), and it may be related to
626 395 stress relaxation, equilibration, and isostatic readjustment after the cease of subduction.

629 396 Antarctica is to a large degree in isostatic equilibrium, although the large basins in West
630 397 Antarctica are slightly undercompensated, and the <S> Transantarctic Mountains and the
631 398 Wilkes Basin are highly undercompensated (*Fig. 11a*). In West Antarctica, free air anomalies
632 399 are slightly positive (+25 mGal) in topographic highs, including the volcanic arc (*Fig. 8a, 11a*).
633 400 The generally slightly negative (-23±20 mGal) free air anomalies in the <N> and <S> West
634 401 Antarctica back-arc basins are superimposed by three NW-SE linear strong negative (ca. -70-
635 402 100 mGal) anomalies within the Ross Ice Shelf that have been interpreted earlier as continental
636 403 rift grabens (*Cooper et al., 1991*). These features do not show up as prominent Bouguer
637 404 anomalies (*Fig. 11b*), and we propose that they are caused by extinct spreading zones in the
638 405 back-arc system.

642 406 Bouguer anomalies also follow the pattern expected for active margins (*Artemieva et al.,*
643 407 *2016*). The transition from oceanic lithosphere to the volcanic arc is marked by a sharp change
644 408 in Bouguer anomalies from >+250 mGal to <+100 mGal (*Fig. 11b*) which coincides with the

650
651
652 409 linear belt of negative free air anomalies and the zone of seismicity. There is a sharp contrast
653 410 in Bouguer anomalies between strongly negative values (-100-250 mGal) in the East Antarctica
654 411 craton and near-zero (-30 to +40 mGal) values in basins of the Ross Ice Shelf and Marie Byrd
655 412 Land, up to ca. +100 mGal in the Ronne Ice Shelf, and ca. -50 mGal in the volcanic arc and in
656 413 the Ellsworth mountains (Fig. 11b). Typically, back-arc basins of the world have stronger
657 414 positive Bouguer anomalies, >+100 mGal, than in West Antarctica (Fig. 9), but some back-arc
658 415 basins, like the Tyrrhenian and the Andaman seas, have Bouguer anomalies in the same range
659 416 of 0-200 mGal as in West Antarctica (Fig. 9; Table 1). We speculate that the amplitude of the
660 417 anomaly reflects the amount of oceanic-type crust that has been produced (that is the maturity
661 418 of back-arc spreading), as well as later compensation by deposited sediments, which form a
662 419 much thicker sequence in West Antarctica than in most other back-arc systems and, therefore,
663 420 reduces the amplitude of the Bouguer gravity anomalies.
664
665
666
667
668

669 421 **5.4. Crustal structure**

670
671 422 A characteristics of back-arc basins is the presence of zones where oceanic-type crust is,
672 423 or is close to, being produced. The West Antarctica basins have thin (25 ± 5.7 km) crust (Fig. 4)
673 424 similar to the back-arc basins of the Aegean Sea, the Okinawa Trough and, possibly, the Sea
674 425 of Japan (Fig. 9). Such widely occurring thin crust is atypical for continental lithosphere except
675 426 for much more localized rift zones (Christensen & Mooney, 1995) and subduction-related back-
676 427 arc basins (Table 1).
677
678

679 428 We observe a strong linear correlation between the equivalent topography and crustal
680 429 thickness (Fig. 12), with the best correlation for the cratonic East Antarctica where Airy-type
681 430 isostatic compensation clearly dominates. The slope of the line determines the average density
682 431 contrast between the crust and the upper mantle (Fig. 13), which is therefore very uniform for
683 432 different tectonic provinces, with compositional variations in crustal density apparently
684 433 compensated by temperature-induced mantle density variations. The predicted density contrast
685 434 between the crust and the upper mantle is ca. 0.35 g/cm^3 (Fig. 13). This value is similar to the
686 435 best fit estimates of Moho density contrast ($0.23\text{-}0.40 \text{ g/cm}^3$) for both East Antarctica craton
687 436 and West Antarctica based on fitting gravity and seismic data on crustal thickness (O'Donnell
688 437 and Nyblade, 2014).
689
690
691

692 438 Back-arc basins of the world follow the same general trend but with a large scatter (Table
693 439 1, Fig. 9), as also the West Antarctica domain. We attribute this scatter to crustal density
694 440 heterogeneity associated with extension, magmatism (in form of sills, diapirs and
695 441 underplating), and metamorphism which are common for back-arc basins, as well as to mantle
696 442 density heterogeneity associated with different stages of back-arc extension.
697
698
699
700

701 443 **6. Continent revisited: West Antarctica lithosphere density model**

702
703 444 We support our interpretation of West Antarctica as a system of back-arc basins by a new
704 445 regional density model of the lithosphere, which shows the presence of a hot low-density
705
706
707
708

709
710
711 446 mantle (Fig. 14a) below most of the West Antarctica. The pattern is in overall agreement with
712 447 lithosphere thermal structure as constrained by airborne magnetic anomalies (Martos *et al.*,
713 448 2017) (Fig. 14b).

715 449 Residual mantle gravity anomalies (Fig. 14a) calculated under the assumption of a
716 450 constant crustal density for all of Antarctica show a sharp distinction between East and West
717 451 Antarctica, with extremely low (<-300 mGal) values in West Antarctica and intermediate to
718 452 high values in the East Antarctic craton. These anomalies require strong thermo-chemical
719 453 heterogeneity of the mantle that may be enhanced by crustal density heterogeneity. We
720 454 examine the relative roles of crustal and mantle heterogeneities and a possible range of in situ
721 455 mantle density values for two end-member scenarios discussed below (Fig. 15). In the absence
722 456 of high-resolution models on the internal velocity and density structure of the crust of most of
723 457 Antarctica (Fig. 4) other approaches are not justified.

728 729 458 **6.1. Model 1: variable crustal density**

730
731 459 Assuming only crustal thickness and density heterogeneity, isostatic compensation at the
732 460 Moho, and an average crustal density of 2.8 g/cm³ at a reference cratonic station, we calculate
733 461 the average crustal density (Fig. 15a) required to explain the Bouguer anomalies (Fig. 11b) for
734 462 the known equivalent topography (Fig. 3) and seismic crustal thickness (Fig. 4). In this scenario,
735 463 we find crustal density in the East Antarctica craton within the normal range for shield crust,
736 464 around 2.8-2.9 g/cm³ (Artemieva and Shulgin, 2019). However, the crust of West Antarctica
737 465 has extremely low predicted average density, between 2.1 and 2.6 g/cm³.

740 466 Average crustal density values of 2.4-2.6 g/cm³ (crystalline basement plus the
741 467 sedimentary cover) are only possible if the sedimentary cover (with average density of ~2.2
742 468 g/cm³) forms ca. 40-60% of the total crustal thickness as in the Peri-Caspian depression
743 469 (Artemieva and Thybo, 2013). For the West Antarctica basins, it would imply that the
744 470 crystalline basement is only ca. 10-12 km thick and the sedimentary cover is ca. 12-15 km
745 471 thick, which is in agreement with seismic observations in the Victoria Land Basin of the Ross
746 472 Subglacial Basin (Cooper *et al.*, 1991), but nearly double of the reported 8 km thickness of
747 473 Mesozoic sediments in other grabens of the Ross Sea (Cooper *et al.*, 1991; Harley, 2003).

750 474 Unrealistically low average crustal density values of <2.4 g/cm³ required by the model
751 475 for Ellsworth Land, the Ross Ice Shelf and the Ross Sea are directly correlated with thin crust
752 476 (Fig. 4). Furthermore, the regions with very low predicted average crustal density are all
753 477 associated with young volcanoes (Fig. 15a), with thin lithosphere as constrained by seismic
754 478 tomography (An *et al.*, 2015a) (Fig. 5a), and with very small Curie depth (Martos *et al.*, 2017)
755 479 (Fig. 14b). We therefore conclude that a significant contribution from the mantle is required to
756 480 explain the Bouguer anomalies in West Antarctica, for example through high mantle
757 481 temperatures, such as expected in back-arc basins.

6.2. Model 2: variable density of lithosphere mantle

As another end-member scenario, we assume that no density heterogeneity exists in the crust with an average density of 2.8 g/cm^3 and that all mantle density anomaly resides in the layer between the Moho and the LAB as defined from a recent regional seismic tomography model (*An et al., 2015b*) (Fig. 5a). In this scenario, we find lithospheric mantle densities at room (SPT) conditions between 3.3 and 3.4 g/cm^3 in the East Antarctic craton and less than 3.1 g/cm^3 in West Antarctica (Fig. 15b) (recalculated from in situ to room temperatures assuming that the seismic LAB corresponds to $1300 \text{ }^\circ\text{C}$). The values for East Antarctica are within the range expected for continental lithosphere mantle (*Griffin et al., 2003*) and in agreement with other results (*Lloyd et al., 2015*) that the Ellsworth-Whitmore mountains have cratonic density values, thus supporting a Precambrian age of these mountains (*Wareham et al., 1998*). The West Antarctica values are extremely low, implying that either average crustal density should also be low, or that lithospheric mantle has very high temperatures with possible presence of fluids and melts. We interpret these low-density mantle anomalies as related to the back-arc spreading, including a possible mid-ocean ridge formation (*Talwani et al., 1965*), which has later ceased as in the Sea of Japan.

The assumption of a constant average crustal density of 2.8 g/cm^3 (crystalline basement plus sediments) in this end-member scenario, together with seismic data on the presence of ca 8 km thick layer of Mesozoic sediments in grabens of the Ross Subglacial Basin (*Cooper et al., 1991; Harley, 2003*) require an average density of $\sim 3.0 \text{ g/cm}^3$ of ca. 12-15 km thick crystalline crust. Such high density requires the presence of high-density underplated material in the lower crust (*Thybo & Artemieva, 2013*) and the absence of a low-density radiogenic granitic layer, which is characteristic of the continental crust. This conclusion again supports our interpretation that a significant part of West Antarctica may have oceanic or transitional crust.

Our results indicate that the most recent back-arc spreading in West Antarctica appears to be concentrated over most of central and <S> West Antarctica, where low-density anomalies indicative of the presence of a hot mantle are located (Fig. 15b). For the Ronne Ice Shelf, the knowledge of crustal structure is insufficient for definite conclusions on the origin of the basin. It also hampers determination of mantle density structure. However, anomalously deep equivalent hypsometry (including the deepest values in West Antarctica, down to $>-1.5 \text{ km}$) together with the results of regional seismic tomography (*Ritzwoller et al., 2001; An et al., 2015a*) indicate a common geodynamic origin of the Ronne Ice Shelf and the Marie Byrd Land - Ross Ice Shelf lithospheric regions.

By analogy between mantle density anomalies beneath West Antarctica and the Wilkes basin in East Antarctica, we propose that the latter may be another back-arc basin that developed when subduction jumped eastwards (*Harley, 2003*) (ca. 86 Ma), to the present day <S> Transantarctic Mountains (Fig. 3b, 16). This conclusion agrees with interpretation of regional aeromagnetic signatures (*Ferraccioli et al., 2001; 2009; Ferraccioli and Bozzo, 2003*) and with flexural models of lithosphere deformation (*Stern & ten Brink 1989; van Wijk et al., 2008*).

6.3. Summary

We conclude, that residual mantle gravity anomalies require the combined effect of:

(1) the absence of a granitic crustal layer and the presence of high density crustal material below a thick sedimentary sequence which makes up to ca. 30-50% of the total crustal thickness, and

(2) the presence of extremely low-density mantle below the basins of West Antarctica and, possibly, below the Wilkes Basin in East Antarctica.

Based on geophysical data on crustal thickness, equivalent topography, mantle residual gravity anomalies, lithosphere thickness, and the spatial-temporal patterns of the volcanic belt, seismicity and free air gravity anomalies, we propose that the basins in West Antarctica developed in back-arc systems (Fig. 16) due to subduction roll-back at various stages. The early formation of the Ronne Ice Shelf basin explains the relatively high lithospheric mantle densities (Fig. 15b) because low temperatures have re-equilibrated after a long cooling history.

7. Continent revisited: Geodynamic setting of the back-arc system

Based on a variety of geophysical evidence and our new lithosphere density model, we have demonstrated that West Antarctica cannot be made of normal continental crust, even if modified by extension to form a large rift system as proposed in early models and commonly accepted until present. The extraordinary deep equivalent hypsometry in West Antarctica is atypical for any continental lithosphere setting (Fig. 6). This first order observation, despite known for more than a decade, demonstrates on its own that a major part of West Antarctica cannot be continental. Our density modelling results, together with regional seismic, geochemical and geological evidence for crustal extension and magmatism, require that West Antarctica instead formed in a back-arc setting, as also further supported by the patterns of seismicity and gravity anomalies (Figs. 3b, 8, 11).

Geochemical data for early- to mid-Cretaceous magmatic rocks from West Antarctica have long been interpreted as subduction-related (sections 3.1-3.3), although with some controversy. Active subduction of the Phoenix Plate along the <W> margin of West Antarctica is generally recognized from plate reconstructions and sampling of subduction-related volcanic rocks (Mukasa and Dalziel, 2000; Weaver et al., 1994). Along Marie Byrd Land, subduction ceased from 108 to 95 Ma (Weaver et al., 1994), while a nearly simultaneous break-up between West Antarctica and Zealandia in Marie Byrd Land initiated rifting-related volcanism as demonstrated by the occurrence of A-type granites (Weaver et al., 1994). However, subduction at the Panthalassic/Pacific margin, gradually ceasing from <S> to <N>, continued along the Antarctic Peninsula so that presently the only remaining active subduction is at the northern tip of the Antarctic Peninsula (at the South Shetland Islands).

These paleo-subduction events formed a magmatic arc along the West Antarctica margin, which includes the Antarctic Peninsula, Ellsworth Land and Marie Byrd Land. However, the

886
887
888
889 560 exact timing of subduction is uncertain due to sparse geochemical sampling in this inaccessible,
890 561 ice-covered region (Fig. 2b). A compilation of the age progression of volcanic rocks based on
891 562 the available limited sampling is summarized in Fig. 3. The uncertainties related to the
892 563 geochemical studies in the region may be illustrated by the difference between an anonymous
893 564 reviewer's comment to our manuscript: "the Marie Byrd Land volcanic rocks contain no
894 565 evidence of a subduction input in their geochemistry", whereas Weaver et al. (1994) and
896 566 Mukasa & Dalziel (2000) provide geochemical evidence for the presence of subduction-related
897 567 volcanic rocks between 320 and 108 Ma in Marie Byrd Land. The uncertainties appear further
898 568 evident from another reviewer's comment: "Along the entire length of the Antarctic Peninsula,
899 569 post-subduction alkaline volcanic rocks occur in scattered locations and these are unusual in
900 570 having no subduction signature", despite it appears clear from other evidence, including
902 571 seismicity (Fig. 3b), that subduction existed.

903
904 572 With sparse geochemical sampling, leading to controversy regarding geodynamic
905 573 interpretations, our results based on geophysical evidence and first order observation of the
906 574 non-continental deep hypsometry of the West Antarctic basins, contribute to constraining
907 575 geodynamic models for the formation and evolution of West Antarctica. Two earlier studies
908 576 are further important for our new interpretation of West Antarctica geodynamics.

910 577 (1) Plate reconstructions of relative movements between East and West Antarctica
911 578 indicate relative rotation that may amount to ca. 180 km of separation in the Eocene and
912 579 Oligocene (Cande et al., 2000).

914 580 (2) Sparse outcrops of locally exposed volcanic rocks in the Ellsworth and Pensacola
915 581 mountains around the edge of the Ronne Ice Shelf (Fig. 2b) formed basis for speculations about
916 582 late Paleozoic – early Mesozoic back-arc basin(s) with an undefined areal extent (Dalziel and
918 583 Elliot, 1982; Collinson et al., 1994).

920 584 Based on our geophysical observations and interpretations, taking into account plate
921 585 reconstructions and the age progression of magmatism and extension in West Antarctica (Fig.
922 586 3a) and by analogy with back-arc basins in the Western Pacific (Van Horne et al., 2015), we
924 587 propose the existence of three rotated back-arc basins caused by differential slab roll-back in
925 588 the Mesozoic associated with subduction of the Phoenix plate under the West Antarctica
926 589 margin (Fig. 7). Our geodynamic model involves four stages:

- 928 590 • **Stage I:** Eastward subduction of the Phoenix plate under what presently makes East
929 591 Antarctica and eastwards movement of lithospheric terranes that later form West Antarctica.
- 930 592 • **Stage II:** Collision between the terranes and East Antarctica, leading to subduction
931 593 jump to the western side of the colliding terranes, probable development of a transform fault
932 594 in the Ross Sea region, reactivation of the Transantarctic mountains, and development of
933 595 subduction-related volcanism at the Antarctic Peninsula and along the margin of Ellsworth
934 596 Land.
- 935 597 • **Stage III:** Slab roll-back and rotational opening of the Ronne Ice Shelf back-arc basin
936 598 with <S>ward progression of arc-related volcanism along the western margin of West
937 599 Antarctica, while further <S>ward back-arc opening is prevented by the Precambrian block
938 600 of the Ellsworth-Whitmore mountains.

945
946
947
948
949
950
951
952
953
954
955
956
957
958
959
960
961
962
963
964
965
966
967
968
969
970
971
972
973
974
975
976
977
978
979
980
981
982
983
984
985
986
987
988
989
990
991
992
993
994
995
996
997
998
999
1000
1001
1002
1003

- 601 • **Stage IV:** Slab roll-back in the central West Antarctica (Marie Byrd Land), leading to
602 rotational opening of the Ross Ice Shelf back-arc basin on the accreted lithosphere and active
603 subduction-related volcanism in the <S>, with further <S> slab roll-back causing extension
604 in the Victoria Land and *possible* formation of the Wilkes back-arc basin on the cratonic
605 lithosphere of East Antarctica.

606 Given the limitations involved in the sampling of volcanic rocks and plate reconstructions
607 in the region, we stress that the timing of these events remains uncertain. However, all
608 geophysical evidence requires that the basin system in West Antarctica originates from
609 Mesozoic back-arc systems. It is possible that the Cenozoic subduction below the Antarctica
610 Peninsula contributed by further back-arc extension in the <N> basins around the Ronne Ice
611 Sheet and the Weddell Sea. Although the back-arc formation has ceased, West Antarctica,
612 which makes one third of the traditionally considered continent, still preserves geophysical and
613 hypsometric characteristics of back-arc systems.

614 **8. Conclusions**

615 We review geophysical and geological observations for West Antarctica and propose that
616 the region traditionally interpreted as the West Antarctic Rift System, together with the Ronne
617 Ice Shelf formed as a system of back-arc basins.

618 1. Our proposed model explains within the same framework the unusually deep
619 equivalent hypsometry of the lithosphere in the West Antarctica superdeep basins, the
620 subduction-related volcanic arc flanking these basins on the ocean side, and the seismicity
621 pattern along the volcanic arc of West Antarctica.

622 2. The calculated mantle residual gravity anomalies and lithosphere mantle density show
623 a strong contrast between the East Antarctic craton and West Antarctica. They require the
624 absence of a granitic crustal layer and the presence of high-density crustal material below a
625 thick sedimentary sequence and the presence of extremely low-density mantle below the basins
626 of West Antarctica and the Wilkes Basin in East Antarctica. These results favor the presence
627 of oceanic or transitional crust in most of West Antarctica and possibly beneath the Ronne Ice
628 Shelf.

629 3. Our model predicts that a granitic crustal layer with a high radiogenic heat production
630 is almost absent in most of West Antarctica, which may affect heat flux at the base of the ice
631 with potential important implications for models of ice melting.

632 4. Importantly, the new geodynamic model reduces the size of the Antarctica continent
633 proper, as 1/3 of its perceived area should be regarded as a back-arc system including deep
634 basins and the volcanic arc instead of extended continental lithosphere.

635 Clearly this new model will open new perspectives for understanding the ice sheet
636 dynamics in Antarctica, which is affected by basal ice melting. It also has significant
637 implications for global models of lithosphere-mantle interaction and lithosphere plate
638 dynamics.

1004
1005
1006
1007
1008
1009
1010
1011
1012
1013
1014
1015
1016
1017
1018
1019
1020
1021
1022
1023
1024
1025
1026
1027
1028
1029
1030
1031
1032
1033
1034
1035
1036
1037
1038
1039
1040
1041
1042
1043
1044
1045
1046
1047
1048
1049
1050
1051
1052
1053
1054
1055
1056
1057
1058
1059
1060
1061
1062

639 **Acknowledgements.** *We appreciate comments of five anonymous reviewers which*
640 *demonstrate substantial controversy in the opinions on geodynamic evolution of West*
641 *Antarctica. These controversial comments guided us when working on the manuscript.*

1063
1064
1065
1066
1067
1068
1069
1070
1071
1072
1073
1074
1075
1076
1077
1078
1079
1080
1081
1082
1083
1084
1085
1086
1087
1088
1089
1090
1091
1092
1093
1094
1095
1096
1097
1098
1099
1100
1101
1102
1103
1104
1105
1106
1107
1108
1109
1110
1111
1112
1113
1114
1115
1116
1117
1118
1119
1120
1121

642 **References**

643 An, M. J. et al. (2015a). Temperature, lithosphere-asthenosphere boundary, and heat flux beneath the
644 Antarctic Plate inferred from seismic velocities. *J. Geophys. Res.*, 120, 8720-8742.

645 An, M. J. et al. (2015b). S-velocity model and inferred Moho topography beneath the Antarctic Plate
646 from Rayleigh waves. *J. Geophys. Res.*, 120, 359-383.

647 Artemieva I.M. and Shulgin A., 2019. Making and altering the crust: A global perspective on crustal
648 structure and evolution. *Earth Planet. Sci. Lett.*, 512, 8-16

649 Artemieva I.M., 2006. Global 1°×1° thermal model TC1 for the continental lithosphere: Implications
650 for lithosphere secular evolution. *Tectonophysics*, 416, 245-277.

651 Artemieva, I. M. & Thybo, H. (2013). EUNaseis: A seismic model for Moho and crustal structure in
652 Europe, Greenland, and the North Atlantic region. *Tectonophysics* 609, 97-153,
653 doi:10.1016/j.tecto.2013.08.004

654 Artemieva, I. M., Thybo, H. & Shulgin, A. (2016). Geophysical constraints on geodynamic processes
655 at convergent margins: A global perspective. *Gondwana Research* 33, 4-23,
656 doi:10.1016/j.gr.2015.06.010

657 Bannister, S., Snieder, R.K., Passier, M.L., 2000. Shear-wave velocities under the Transantarctic
658 Mountains and Terror Rift from surface wave inversion. *Geophys. Res. Lett.* 27, 281– 284.

659 Baranov, A. & Morelli, A. (2013). The Moho depth map of the Antarctica region. *Tectonophysics*
660 609, 299-313.

661 Barker, P.F. (1982). The Cenozoic subduction history of the Pacific margin of the Antarctic
662 Peninsula: ridge crest–trench interactions. *J. Geol. Soc. London* 139, 787-801.

663 Behrendt, J. C. (1999). Crustal and lithospheric structure of the West Antarctic Rift System from
664 geophysical investigations — a review. *Global and Planetary Change* 23, 25-44.

665 Behrendt, J. C. (2013). The aeromagnetic method as a tool to identify Cenozoic magmatism in the
666 West Antarctic Rift System beneath the West Antarctic Ice Sheet - A review; Thiel subglacial
667 volcano as possible source of the ash layer in the WAISCOPE. *Tectonophysics* 585, 124-136.

668 Behrendt, J. C., LeMasurier, W.E., Cooper, A.K., Tessensohn, F., Trehu, A. & Damaske, D. (1991).
669 Geophysical studies of the west Antarctica rift system. *Tectonics* 10, 1257-1273.

670 Behrendt, J.C., Blankenship, D.D., Damaske, D., Cooper, A.K., Finn, C., Bell, R.E., 1997.
671 Geophysical evidence for late Cenozoic subglacial volcanism beneath the West Antarctic Ice Sheet
672 and additional speculation as to its origin. In: *The Antarctic Region: Geological Evolution and*
673 *Processes*, 539–546.

674 Behrendt, J.C., Blankenship, D.D., Finn, C.A., Bell, R.E., Sweeney, R.E., Hodge, S.R., Brozena, J.M.,
675 1994. Evidence for late Cenozoic Flood Basalts (?) in the West Antarctic Rift System revealed by
676 the CASERTZ Aeromagnetic Survey. *Geology* 22, 527–530.

677 Bingham, R. G. et al. (2012). Inland thinning of West Antarctic Ice Sheet steered along subglacial
678 rifts. *Nature* 487, 468-471.

679 Blankenship, D.D., Bell, R.E., Hodge, S.M., Brozena, J.M., Behrendt, J.C., Finn, C.A., 1993. Active
680 volcanism beneath the West Antarctic Ice Sheet. *Nature* 361, 526–529.

681 Block, A.E., Bell, R.E. & Studinger, M. (2009). Antarctic crustal thickness from satellite gravity:
682 implications for the Transantarctic and Gamburtsev Subglacial Mountains, *Earth planet. Sci. Lett.*,
683 288, 194–203.

684 Boger S.D., 2011. Antarctica — Before and after Gondwana. *Gondwana Research*, 19, 335-371.

685 Bradshaw, J.D., 1989. Cretaceous geotectonic patterns in the New Zealand region. *Tectonics* 8, 803–
686 820.

687 Brooks, D. A. et al. (1984). Characteristics of back-arc regions. *Tectonophysics* 102, 1-16.

688 Busetti, M., Spadini, G., Van der Wateren, F.M., Cloetingh, S. & Zanolla, C., 1999. Kinematic
689 modelling of the west Antarctic rift system, Ross Sea, Antarctica, *Global Planet. Change*, 23, 79–
690 103.

691 Cande, S. C., and J. M. Stock (2004), Cenozoic reconstructions of the Australia-New Zealand-South
692 Pacific sector of Antarctica, in *The Cenozoic Southern Ocean: Tectonics, Sedimentation, and*
693 *Climate Change Between Australia and Antarctica*, pp. 5–17, AGU, Washington, D. C.

- 1122
1123
1124 694 Cande, S. C., Stock, J. M., Muller, R. D. & Ishihara, T. (2000). Cenozoic motion between East and
1125 695 West Antarctica. *Nature* 404, 145-150.
- 1126 696 Chaput, J., R. C. Aster, A. Huerta, X. Sun, A. Lloyd, D. Wiens, A. Nyblade, S. Anandkrishnan, J. P.
1127 697 Winberry, and T. Wilson (2014), The crustal thickness of West Antarctica, *J. Geophys. Res.*, 119,
1128 698 378–395.
- 1129 699 Christensen, N. I. & Mooney, W. D. (1995). Seismic velocity structure and composition of the
1130 700 continental crust; a global view. *J. Geophys. Res.*, 100, 9761-9788
- 1131 701 Christeson, G. L. et al. (2014). Deep crustal structure in the eastern Gulf of Mexico. *Journal of*
1132 702 *Geophysical Research-Solid Earth* 119, 6782-6801, doi:10.1002/2014jb011045
- 1133 703 Collinson, J. W. et al. (1994). Permian-Triassic Transantarctic basin. *Geological Society of America*
1134 704 *Memoirs* 184, 173-222
- 1135 705 Cooper, A. K. and Davey, F. J. (1985). Episodic rifting of Phanerozoic rocks in the Victoria Land
1136 706 Basin, western Ross Sea, Antarctica. *Science* 229, 1085–1087.
- 1137 707 Cooper, A. K. et al. (1991). Cenozoic prograding sequences of the Antarctic continental-margin - a
1138 708 record of glacioeustatic and tectonic events. *Marine Geology* 102, 175-213.
- 1139 709 Cooper, A.K., Barker, P.F., Branconlini Eds., 1995. *Geology and Seismic Stratigraphy of the*
1140 710 *Antarctic Margin*. Antarctic Research Series 68, American Geophysical Union, 303 pp.
- 1141 711 Crawford, W. C., Wiens, D. A., Dorman, L. M., Webb, S. C. & Wiens, D. A. (2003). Tonga Ridge
1142 712 and Lau Basin crustal structure from seismic refraction data. *Journal of Geophysical Research-*
1143 713 *Solid Earth* 108, doi:10.1029/2001jb001435
- 1144 714 Dalziel, I. W., L. A. Lawver, I. O. Norton, and L. M. Gahagan (2013), The Scotia Arc: Genesis,
1145 715 evolution, global significance, *Annu. Rev. Earth Planet. Sci.*, 41, 767–793.
- 1146 716 Dalziel, I.W.D. (1992). Antarctica; a tale of two supercontinents? *Annu. Rev. Earth Planet. Sci.*, 20:
1147 717 501-526.
- 1148 718 Darniani, T. M., Jordan, T. A., Ferraccioli, F., Young, D. A. & Blankenship, D. D. (2014). Variable
1149 719 crustal thickness beneath Thwaites Glacier revealed from airborne gravimetry, possible
1150 720 implications for geothermal heat flux in West Antarctica. *Earth and Planetary Science Letters* 407,
1151 721 109-122.
- 1152 722 Davey, F. J. et al. (2016). Synchronous oceanic spreading and continental rifting in West Antarctica.
1153 723 *Geophysical Research Letters* 43, 6162-6169.
- 1154 724 Dickinson, W. R. Plate tectonic evolution of North Pacific Rim. *J.Phys.Earth* 26, S1-S19 (1978).
- 1155 725 Dietz, R. S., and W. P. Sproll, 1970. Fit between Africa and Antarctica: A continental drift
1156 726 reconstruction. *Science*, 167, 1612-1614.
- 1157 727 Eagles G., R.D. Larter, K. Gohl, & A.P.M. Vaughan, 2009. West Antarctic Rift System in the
1158 728 Antarctic Peninsula. *Geophys. Res. Lett.*, 36(21) DOI: 10.1029/2009GL040721
- 1159 729 Ebbing J., P. Haas, F. Ferraccioli, F. Pappa, W. Szwillus & J. Bouman, 2018. Earth tectonics as seen
1160 730 by GOCE -Enhanced satellite gravity gradient imaging. *Sci. Rep.*, 8:16356 | DOI:10.1038/s41598-
1161 731 018-34733-9
- 1162 732 Faure G. and Mening T.M., 2010,. *The Transantarctic Mountains: Rocks, Ice, Meteorites and Water*,
1163 733 Springer, 832 pp..
- 1164 734 Fei Ji, Fei Li, Jin-Yao Gao, Qiao Zhang, Wei-Feng Hao (2018). 3-D density structure of the Ross Sea
1165 735 basins, West Antarctica from constrained gravity inversion and their tectonic implications.
1166 736 *Geophysical Journal International*, 215, 1241–1256.
- 1167 737 Feng, M. et al. (2014). Crustal thicknesses along the traverse from Zhongshan to Dome A in Eastern
1168 738 Antarctica. *Chin. J. Polar Res.* 26, 177-185
- 1169 739 Ferraccioli, F. & Bozzo, E. (2003). Cenozoic strike-slip faulting from the eastern margin of the
1170 740 Wilkes Subglacial Basin to the western margin of the Ross Sea Rift: an aeromagnetic connection.
1171 741 *Geological Society, London, Special Publications* 210, 109-133.
- 1172 742 Ferraccioli, F. et al. (2001). Rifting(?) crust at the East Antarctic Craton margin: gravity and magnetic
1173 743 interpretation along a traverse across the Wilkes Subglacial Basin region. *Earth and Planetary*
1174 744 *Science Letters* 192, 407-421.
- 1175 745 Ferraccioli, F., Armadillo, E., Jordan, T., Bozzo, E., Corr, H., 2009. Aeromagnetic exploration over
1176 746 the East Antarctic Ice Sheet: A new view of the Wilkes Subglacial Basin. *Tectonophysics* 478, 62-
1177 747 77.

1181
1182
1183
1184
1185
1186
1187
1188
1189
1190
1191
1192
1193
1194
1195
1196
1197
1198
1199
1200
1201
1202
1203
1204
1205
1206
1207
1208
1209
1210
1211
1212
1213
1214
1215
1216
1217
1218
1219
1220
1221
1222
1223
1224
1225
1226
1227
1228
1229
1230
1231
1232
1233
1234
1235
1236
1237
1238
1239

748 Ferraccioli, F., Finn, C.A., Jordan, T.A., Bell, R.E., Anderson, L.M., Damaske, D., 2011. East
749 Antarctic rifting triggers uplift of the Gamburtsev Mountains. *Nature* 479, 388–392.

750 Ferraccioli, F., Jones, P.C., Vaughan, A.P.M., Leat, P.T., 2006. New aerogeophysical view of the
751 Antarctic Peninsula: More pieces, less puzzle. *Geophysical Research Letters* 33.

752 Finn, C. A., R. D. Müller, and K. S. Panter (2005), A Cenozoic diffuse alkaline magmatic province
753 (DAMP) in the southwest Pacific without rift or plume origin, *Geochem. Geophys. Geosyst.*, 6,
754 Q02005, doi:10.1029/2004GC000723.

755 Fitzgerald, P., Baldwin, S., 1997. Detachment fault model for the evolution of the Ross Embayment.
756 In: Ricci, C.A. (Ed.), *The Antarctic Region: Geological Evolution and Processes*, pp. 555–564.

757 Fitzgerald, P.G., 1992. The Transantarctic Mountains of southern Victoria Land: the application of
758 apatite fission track analysis to a rift shoulder uplift. *Tectonics* 11, 634–662.

759 Fitzsimons, I.C.W. (2000). A review of tectonic events in the East Antarctic Shield and their
760 implications for Gondwana and earlier supercontinents. *Journal African Earth Sciences*, 31, 3-23.

761 Fox Maule, C., Purucker, M. E., Olsen, N., & Mosegaard, K. (2005). Heat flux anomalies in
762 Antarctica revealed by satellite magnetic data. *Science*, 309(5733), 464–467.

763 Fretwell, P. et al. (2013). Bedmap2: improved ice bed, surface and thickness datasets for Antarctica.
764 *Cryosphere* 7, 375-393.

765 Goodman, D., Bibee, L. D. & Dorman, L. M. (1989). Crustal seismic structure beneath the west
766 Philippine Sea, 17-degrees-18-degrees north. *Marine Geophysical Researches* 11, 155-168

767 Granot, R., Cande, S.C., Stock, J.M., Davey, F.J., Clayton, R.W., 2010. Postspreading rifting in the
768 Adare Basin, Antarctica: regional tectonic consequences. *Geochem. Geophys. Geosyst.* 11.
769 <http://dx.doi.org/10.1029/2010GC003105>.

770 Granot, R. & Dymant, J. (2018). Late Cenozoic unification of East and West Antarctica. *Nature*
771 *Communications*, 9, 3189, DOI: 10.1038/s41467-018-05270-w

772 Griffin, W. L. et al. (2003). The origin and evolution of Archean lithospheric mantle. *Precambrian*
773 *Research* 127, 19-41.

774 Hansen S.E., Graw J.H., Kenyon L.M., Nyblade A.A., Wiens D.A., et al. (2014). Imaging the
775 Antarctic mantle using adaptively parameterized P-wave tomography: Evidence for heterogeneous
776 structure beneath West Antarctica. *Earth and Planetary Science Letters*, 408, 66-78

777 Hansen, S.E., Kenyon, L.M., Graw, J.H., Park, Y. & Nyblade, A.A., 2016. Crustal structure beneath
778 the Northern Transantarctic Mountains and Wilkes Subglacial Basin: implications for tectonic
779 origins, *J. Geophys. Res.*, 121, 812–825.

780 Harley, S. L. (2003). The geology of Antarctica, in *Encyclopedia of Life Support Systems (EOLSS)*
781 *Vol. IV* (eds Benedetto De Vivo, Kurt Stuwe, & Bernhard Grasemann) (The UNESCO, Eolss
782 Publishers [<http://www.eolss.net>] Paris, France, 2003).

783 Hart, S.R., Blusztajn, J., Le Masurier, W.E., Rex, D.C., 1997. Hobbs Coast Cenozoic volcanism:
784 implications for the West Antarctic rift system. *Chem. Geol.* 139, 223–248

785 Houtz, R. & Davey, F.J., 1973. Seismic profiler and sonobuoy measurements in Ross Sea, Antarctica,
786 *J. geophys. Res.*, 78, 3448–3468.

787 Huerta, A.D. & Harry, D.L., 2007. The transition from diffuse to focused extension: modeled
788 evolution of the West Antarctic Rift system, *Earth planet. Sci. Lett.*, 255, 133–147.

789 Iwasaki, T., Levin, V., Nikulin, A. & Idaka, T. (2013). Constraints on the Moho in Japan and
790 Kamchatka. *Tectonophysics* 609, 184-201.

791 Jankowski, E.J. & Drewry, D.J. 1981 . The structure of West Antarctica from geophysical studies.
792 *Nature* 291: 1 7-21

793 Jordan, T. A., F. Ferraccioli, D. G. Vaughan, J. W. Holt, H. Corr, D. D. Blankenship, and T. M. Diehl
794 (2010), Aerogravity evidence for major crustal thinning under the Pine Island Glacier region (West
795 Antarctica), *Geol. Soc. Am. Bull.*, 122(5–6), 714–726.

796 Jordan, T. A., Ferraccioli, F. & Leat, P. T. (2017). New geophysical compilations link crustal block
797 motion to Jurassic extension and strike-slip faulting in the Weddell Sea Rift System of West
798 Antarctica. *Gondwana Research* 42, 29-48.

799 Jordan, T.A., Ferraccioli, F., Armadillo, E., Bozzo, E., 2013. Crustal architecture of the Wilkes

1240
1241
1242 800 Karner, G.D., Studinger, M., Bell, R.E., 2005. Gravity anomalies of sedimentary basins and their
1243 801 mechanical implications: application to the Ross Sea basins, West Antarctica. *Earth Planet. Sci.*
1244 802 *Lett.* 235, 577–596.
1245 803 König M. & Jokat W. (2006). The Mesozoic breakup of the Weddell Sea. *J. Geophys. Res.*, 111,
1246 804 B12102.
1247 805 Kyle, P. R. & Muncy, H. L. (1989). Geology and geochronology of McMurdo volcanic group rocks in
1248 806 the vicinity of Lake Morning, McMurdo Sound, Antarctica. *Antarctic Science* 1, 345-350
1249 807 Larter, R. D. & Barker, P. F. (1991). Effects of ridge crest-trench interaction on Antarctic Phoenix
1250 808 spreading - forces on a young subducting plate. *J. Geophysical Res.* 96, 19583-19607.
1251 809 Larter, R.D., Cunningham, A.P., Barker, P.F., Gohl, K., Nitsche, F.O. (2002). Tectonic evolution of
1252 810 the Pacific margin of Antarctica, 1. Late Cretaceous tectonic reconstructions. *Journal of*
1253 811 *Geophysical Research* 107, 2345. doi:10.1029/2000JB000052.
1254 812 Lawver, L.A. & Gahagan, L.M., 1994. Constraints on timing of extension in the Ross Sea Region.
1255 813 *Terra Antarctica* 1, 545–552.
1256 814 Lawver, L.A., Royer, J.Y., Sandwell, D.T., Scotese, C.R., 1991. Evolution of the Antarctic
1257 815 continental margin. In: Thomson, M., Crame, J., Thomson, J. (Eds.), *Geological Evolution of*
1258 816 *Antarctica*. Cambridge Univ. Press, New York, pp.533–539.
1259 817 Lemasurier, W. E. & Rex, D. C. (1989). Evolution of linear volcanic ranges in Marie Byrd Land,
1260 818 West Antarctica. *Journal of Geophysical Research-Solid Earth and Planets* 94, 7223-7236.
1261 819 LeMasurier, W., 2008. Neogene extension and basin deepening in the West Antarctic rift inferred
1262 820 from comparisons with the East African rift and other analogs. *Geology*, 36, 247–250.
1263 821 LeMasurier, W.E., 1990. Late Cenozoic volcanism on the Antarctic plate: an overview. In:
1264 822 LeMasurier, W.E., Thomson, J.W. Eds., *Volcanoes of the Antarctic plate and southern oceans*.
1265 823 *Antarctic Research Series* 48, American Geophysical Union, Washington, DC, pp. 1–19.
1266 824 Lloyd, A.J., D.A. Wiens, A.A. Nyblade, S. Anandakrishnan, R.C. Aster, A.D. Huerta, T.J. Wilson,
1267 825 I.W.D. Dalziel, P.J. Shore, & D. Zhao (2015), A seismic transect across West Antarctica: Evidence
1268 826 for mantle thermal anomalies beneath the Bentley Subglacial Trench and the Marie Byrd Land
1269 827 Dome, *J. Geophys. Res.*, 120, 8439-8460.
1270 828 Luyendyk B.P., 1995. Hypothesis for Cretaceous rifting of east Gondwana caused by subducted slab
1271 829 capture. *Geology*, 23, 373-376
1272 830 Luyendyk, B., Cisowski, S., Smith, C., Richard, S., Kimbrough, D., 1996. Paleomagnetic study of
1273 831 northern Ford Ranges, western Marie Byrd Land, West Antarctica: motion between West and East
1274 832 Antarctica. *Tectonics* 15, 122–141.
1275 833 Martos, Y. M., Catalán, M., Jordan, T. A., Golynsky, A., Golynsky, D., Eagles, G., & Vaughan, D. G.
1276 834 (2017). Heat flux distribution of Antarctica unveiled. *Geophysical Research Letters*, 44. doi
1277 835 10.1002/2017GL075609
1278 836 McKenzie, D. (1978). Some remarks on the development of sedimentary basins. *Earth Planet. Sci.*
1279 837 *Lett.* 40, 25–32
1280 838 Millar I.A. & Storey B.C. (1995). Early Paleozoic rather than Neoproterozoic volcanism and rifting
1281 839 withing the Transantarctic Mountains. *J Geol Soc London* 152:417–460.
1282 840 Morelli, A., Danesi, S., 2004. Seismological imaging of the Antarctic continental lithosphere: a
1283 841 review. *Glob. Planet. Change*, 42, 155–165
1284 842 Mukasa, S. B. & Dalziel, I. W. D. (2000). Marie Byrd Land, West Antarctica: Evolution of
1285 843 Gondwana's Pacific margin constrained by zircon U-Pb geochronology and feldspar common-Pb
1286 844 isotopic compositions. *Geological Society of America Bulletin* 112, 611-627.
1287 845 Nakamura, M. & Umedu, N. (2009). Crustal thickness beneath the Ryukyu arc from travel-time
1288 846 inversion. *Earth Planets and Space* 61, 1191-1195
1289 847 O'Donnell J.P. & Nyblade A.A., 2014. Antarctica's hypsometry and crustal thickness: Implications
1290 848 for the origin of anomalous topography in East Antarctica. *Earth Planet. Sci. Lett.*, 388, 143-155.
1291 849 Olsen, K. H. (1995). Continental rifts, in *Development in Geophysics* Vol. 25 (Elsevier, Amsterdam).
1292 850 Pavlis, N. K., Holmes, S. A., Kenyon, S. C. & Factor, J. K. (2012). The development and evaluation
1293 851 of the Earth Gravitational Model 2008 (EGM2008). *Journal of Geophysical Research-Solid Earth*
1294 852 117, doi:10.1029/2011jb008916

1299
1300
1301
1302
1303
1304
1305
1306
1307
1308
1309
1310
1311
1312
1313
1314
1315
1316
1317
1318
1319
1320
1321
1322
1323
1324
1325
1326
1327
1328
1329
1330
1331
1332
1333
1334
1335
1336
1337
1338
1339
1340
1341
1342
1343
1344
1345
1346
1347
1348
1349
1350
1351
1352
1353
1354
1355
1356
1357

- 853 Podladchikov, Y.Y., Poliakov, A.N.B., Yuen, D.A., 1994. The effect of lithospheric phase transitions
854 on subsidence of extending continental lithosphere. *Earth Planet. Sci. Lett.* 124, 95–103
- 855 Press, F., Dewart, D., 1959. Extent of the Antarctic Continent. *Science* 129, 462–463.
- 856 Ramirez, C. et al. (2016). Crustal and upper-mantle structure beneath ice-covered regions in
857 Antarctica from S-wave receiver functions and implications for heat flow. *Geophysical Journal*
858 *International* 204, 1636-1648, doi:10.1093/gji/ggv542
- 859 Riley, T. R. & Leat, P. T. (1999). Large volume silicic volcanism along the proto-Pacific margin of
860 Gondwana: lithological and stratigraphical investigations from the Antarctic Peninsula. *Geological*
861 *Magazine* 136, 1-16, doi:10.1017/s0016756899002265
- 862 Ritzwoller, M. H., Shapiro, N. M., Levshin, A. L. & Leahy, G. M. (2001). Crustal and upper mantle
863 structure beneath Antarctica and surrounding oceans. *J. Geophys. Res.* 106, 30645–30670.
- 864 Rocchi, S., Armienti, P., D’Orazio, M., Tonarini, S., Wibrans, J.R., Vincenzo, G.D., 2002. Cenozoic
865 magmatism in the western Ross Embayment: role of mantle plume versus plate dynamics in the
866 development of the West Antarctic Rift System. *J. Geophys. Res.* 107, doi
867 10.1029/2001JB000515.
- 868 Rocchi, S., Armienti, P., Di Vincenzo, G., 2005. No plume, no rift magmatism in the West Antarctic
869 Rift. In: Foulger, G.R., Natland, J.H., Presnall, D.C., Anderson, D.L. (Eds.), *Plates, Plumes, and*
870 *Paradigms*. In: *Geol. Soc. Am. Spec. Paper*, vol.388, pp.435–447.
- 871 Rocchi, S., Storti, F., Di Vincenzo, G., Rosetti, F., 2003. Intraplate strike-slip tectonics as an
872 alternative to mantle plume activity for the Cenozoic rift magmatism in the Ross Sea region,
873 Antarctica. In: Storti, F., Holdsworth, R.E., Salvini, F. (Eds.), *Intraplate Strike-Slip Deformation*
874 *Belts*. *Geol. Soc. (Lond.) Spec. Publ.* 210, 145–158.
- 875 Salvini, F., Brancolini, G., Busetti, M., Storti, F., Mazzarini, F. & Coren, F., 1997. Cenozoic
876 geodynamics of the Ross Sea region, Antarctica: crustal extension, intraplate strike-slip faulting,
877 and tectonic inheritance, *J. Geophys. Res.*, 102, 24669–24696.
- 878 Sartori, R. et al. (2004). Crustal features along a W-E Tyrrhenian transect from Sardinia to Campania
879 margins (Central Mediterranean). *Tectonophysics* 383, 171-192.
- 880 Scheinert, M. et al. (2016). New Antarctic gravity anomaly grid for enhanced geodetic and
881 geophysical studies in Antarctica. *Geophysical Research Letters* 43, 600-610.
- 882 Sengör, A. M. C. & Burke, K. (1978). Relative timing of rifting and volcanism on earth and its
883 tectonic implications. *Geophys. Res. Lett.* 5, 419-421, doi:10.1029/GL005i006p00419
- 884 Seroussi, H., Ivins, E. R., Wiens, D. A. & Bondzio, J. (2017). Influence of a West Antarctic mantle
885 plume on ice sheet basal conditions. *J. Geophys. Res.*, <https://doi.org/10.1002/2017JB014423>
- 886 Shapiro, N. M., & Ritzwoller, M. H. (2004). Inferring surface heat flux distributions guided by a
887 global seismic model: Particular application to Antarctica. *Earth and Planetary Science Letters*,
888 223, 213–224.
- 889 Siddoway, C. S. (2008). Tectonics of the West Antarctic Rift System: New light on the history and
890 dynamics of distributed intracontinental extension, in: Cooper A. K. et al. (Eds.) “Antarctica: A
891 Keystone in a Changing World”, pp. 91-114, The Natl. Acad. Press, Washington, D. C.
- 892 Siddoway, C.S., Baldwin, S.L., Fitzgerald, P.G., Fanning, C.M. & Luyendyk, B.P., 2004. Ross Sea
893 mylonites and the timing of intracontinental extension within the West Antarctic rift system,
894 *Geology*, 32, 57–60.
- 895 Sieminski, A., Debayle, E., Leveque, J.-J., 2003. Seismic evidence for deep low-velocity anomalies in
896 the transition zone beneath West Antarctica. *Earth Planet. Sci. Lett.* 216, 645–661.
- 897 Spasojevic, S., Gurnis, M., and Sutherland, R. (2010), Inferring mantle properties with an evolving
898 dynamic model of the Antarctica-New Zealand region from the Late Cretaceous, *J. Geophys. Res.*,
899 115, B05402, doi:10.1029/2009JB006612.
- 900 Stern, T.A., ten Brink, U.S., 1989. Flexural uplift of the Transantarctic Mountains. *J. Geophys. Res.*
901 94, 10315–10330.
- 902 Stock, J., Molnar, P., 1987. Revised history of early Tertiary plate motion in the south–west Pacific.
903 *Nature* 325, 495–499.
- 904 Storey, B.C., Garrett, S.W. (1985). Crustal growth of the Antarctic Peninsula by accretion,
905 magmatism and extension. *Geological Magazine* 122, 5-14 10.1017/s0016756800034038.

1358
1359
1360 906 Storey, B. C. & Alabaster, T. (1991). Tectonomagmatic controls on Gondwana break-up models -
1361 907 Evidences from the proto-Pacific margin of Antarctica. *Tectonics* 10, 1274-1288.
1362 908 Storey, B. C. et al. (1988). West Antarctica in Gondwanaland - Crustal blocks, reconstruction and
1363 909 breakup processes. *Tectonophysics* 155, 381-390.
1364 910 Storey, B.C. (1996). Microplates and mantle plumes in Antarctica. *Terra Antarctica* 3, 91-102
1365 911 Studinger, M., Bell, R.E., Finn, C.A., Blankenship, D.D., 2002. Mesozoic and Cenozoic extensional
1366 912 tectonics of the West Antarctic Rift system from high-resolution air-borne geophysical mapping.
1367 913 *Bull. R. Soc. N. Z.* 35, 563–569.
1368 914 Subglacial Basin in East Antarctica, as revealed from airborne gravity data. *Tectonophysics* 585, 196-
1369 915 206.
1370 916 Sutherland, R., S. Spasojevic, and M. Gurnis (2010), Mantle upwelling after Gondwana subduction
1371 917 death may explain anomalous topography of West Antarctica and subsidence history of eastern
1372 918 New Zealand, *Geology*, 38, 155–158.
1373 919 Takahashi, N. et al. (2007). Crustal structure and evolution of the Mariana intra-oceanic island arc.
1374 920 *Geology* 35, 203-206, doi:10.1130/g23212a.1
1375 921 Talwani, M., Lepichon, X. and Ewing, M. (1965). Crustal structure of mid-ocean ridges. 2.
1376 922 Computed model from gravity and seismic refraction data. *J. Geophys. Res.*, 70, 341-358.
1377 923 ten Brink, U.S., Hackney, R.I., Bannister, S., Stern, T.A., Makovsky, Y., 1997. Uplift of the
1378 924 Transantarctic Mountains and the bedrock beneath the East Antarctic ice sheet. *J. Geophys. Res.*
1379 925 102, 27603– 27621
1380 926 Thybo, H. & Artemieva, I. M. (2013). Moho and magmatic underplating in continental lithosphere.
1381 927 *Tectonophysics*, 609, 605-619.
1382 928 Thybo, H. & Nielsen, C. A. (2009). Magma-compensated crustal thinning in continental rift zones.
1383 929 *Nature*, 457, 873-876.
1384 930 Tingey R.J., (1991). *The Geology of Antarctica*, Oxford University Press, Oxford.
1385 931 Trey, H., A. K. Cooper, G. Pellis, B. della Vedova, G. Cochrane, G. Brancolini, and J. Makris (1999),
1386 932 Transect across the West Antarctic rift system in the Ross Sea, Antarctica. *Tectonophysics*, 301,
1387 933 61–74.
1388 934 USGS catalogue, <https://earthquake.usgs.gov/earthquakes/search/>.
1389 935 Uyeda, S. & Kanamori, H. (1979). Back-arc opening and the mode of subduction. *Journal of*
1390 936 *Geophysical Research* 84, 1049-1061, doi:10.1029/JB084iB03p01049
1391 937 Van Horne, A., Sato, H. & Ishiyama, T. (2015). Evolution of the Sea of Japan back-arc and some
1392 938 unsolved issues. *Tectonophysics* 644, 58-67.
1393 939 van Wijk, J.W., Lawrence, J.F. & Driscoll, N.W. (2008). Formation of the Transantarctic Mountains
1394 940 related to extension of the West Antarctic rift system, *Tectonophysics*, 458, 117–126.
1395 941 Vaughan A.P.M. and Pankhurst R.J. (2008). Tectonic overview of the West Gondwana margin.
1396 942 *Gondwana Research*, 13, 150-162
1397 943 Vaughan, A. P. M. & Storey, B. C. (2000). The eastern Palmer Land shear zone: a new terrane
1398 944 accretion model for the Mesozoic development of the Antarctic Peninsula. *Journal of the*
1399 945 *Geological Society* 157, 1243-1256
1400 946 Vaughan, A.P.M., Pankhurst, R.J., Fanning, C.M. (2002). Amid-Cretaceous age for the Palmer Land
1401 947 event, Antarctic Peninsula: implications for terrane accretion timing and Gondwana
1402 948 palaeolatitudes. *Journal of the Geological Society of London* 159, 113–116.
1403 949 Weaver, S.D., Storey, B., Pankhurst, R.J., Mukasa, S.B., Divenere, V.J., Bradshaw, J.D. (1994).
1404 950 Antarctica New-Zealand rifting and Marie-Byrd-Land lithospheric magmatism linked to ridge
1405 951 subduction and mantle plume activity. *Geology* 22, 811-814, 10.1130/0091-7613.
1406 952 Veevers, J.J., Powell, C.M., Roots, S.R. (1991). Review of seafloor spreading around Australia. I.
1407 953 Synthesis of the patterns of spreading. *Australian Journal of Earth Sciences* 38, 373–389
1408 954 Veevers, J. J. (2012), Reconstructions before rifting and drifting reveal the geological connections
1409 955 between Antarctica and its conjugates in Gondwanaland, *Earth Sci. Rev.*, 111(3), 249–318.
1410 956 Wannamaker, P.E., Stodt, J.A., & Olsen, S.L., 1996. Dormant state of rifting below the Byrd
1411 957 Subglacial Basin, West Antarctica, implied by magnetotelluric (MT) profiling. *Geophys. Res. Lett.*
1412 958 23, 2983–2986.

1417
1418
1419 959 Wareham, C. D. et al. (1998). Pb, Nd, and Sr isotope mapping of Grenville-age crustal provinces in
1420 960 Rodinia. *Journal of Geology* 106, 647-659
1421 961 Waschbusch, P. & Beaumont, C. (1996). Effect of a retreating subduction zone on deformation in
1422 962 simple regions of plate convergence. *Journal of Geophysical Research-Solid Earth* 101, 28133-
1423 963 28148, doi:10.1029/96jb02482
1424 964 Weaver, S. D., C. J. Adams, R. J. Pankhurst, & I. L. Gibson. 1992. Granites of Edward VII Peninsula,
1425 965 Marie Byrd Land: Anorogenic magmatism related to Antarctic-New Zealand rifting. In Proc. of
1426 966 the Second Hutton Symposium on the Origin of Granites and Related Rocks, eds. E. Brown and B.
1427 967 W. Chappell. *Transactions of the Royal Society of Edinburgh, Earth Sciences* 83:281-290.
1428 968 Weaver, S.D., Storey, B., Pankhurst, R.J., Mukasa, S.B., Divenere, V.J., & Bradshaw, J.D., 1994.
1429 969 Antarctica–New Zealand rifting and Marie Byrd Land lithospheric magmatism linked to ridge
1430 970 subduction and mantle plume activity. *Geology* 22, 811–814.
1431 971 Wernicke, B. (1981). Low-angle normal faults in the Basin and Range Province; nappe tectonics in an
1432 972 extending orogen. *Nature*, 291, 645-648
1433 973 White-Gaynor, A.L., Nyblade, A.A., Aster, R.C., Wiens, D.A., Bromirski, P.D., Gerstoft, P., Stephen,
1434 974 R.A., Hansen, S.E., Wilson, T., Dalziel, I.W., Huerta, A.D., Winberry, J.P., Anandkrishnan, S.,
1435 975 2019, Heterogeneous upper mantle structure beneath the Ross Sea Embayment and Marie Byrd
1436 976 Land, West Antarctica, revealed by P-wave tomography. *Earth and Planetary Science Letters*, 513,
1437 977 40-50, doi: 10.1016/j.epsl.2019.02.013.
1438 978 Wilson, T. J.; Bevis, M.; Konfal, S., et al., 2015. Understanding glacial isostatic adjustment and ice
1439 979 mass change in Antarctica using integrated GPS and seismology observations. *European*
1440 980 *Geophysical Union Annual Meeting Supplement*, 2015EGUGA..17.7762W
1441 981 Winberry, P.J., Anandkrishnan, S., 2004. Crustal structure of the West Antarctic rift system and
1442 982 Marie Byrd Land hotspot. *Geology* 32, 977–980
1443 983 Worner, 1999. Lithospheric dynamics and mantle sources of alkaline magmatism of the Cenozoic
1444 984 West Antarctic Rift System. *Glob. Planet. Change* 23, 61– 77.
1445 985 Zhao, G., Cawood, P.A., Wilde, S.A. & Sun, M. (2002). Review of global 2.1–1.8 Ga orogens:
1446 986 implications for a pre-Rodinia supercontinent. *Earth-Science Reviews*, 59, 125–162
1447 987 Zhu, L. P., Mitchell, B. J., Akyol, N., Cemen, I. & Kekovali, K. (2006). Crustal thickness variations in
1448 988 the Aegean region and implications for the extension of continental crust. *Journal of Geophysical*
1449 989 *Research-Solid Earth* 111, doi:10.1029/2005jb003770
1450 990
1451
1452
1453
1454
1455
1456
1457
1458
1459
1460
1461
1462
1463
1464
1465
1466
1467
1468
1469
1470
1471
1472
1473
1474
1475

Figure Captions

Fig. 1. Basement topography (a) and topography of the ice sheet (b) in the Antarctic region.

Fig. 2. (a) Classic concept of Antarctica consisting of three domains: West Antarctica made of several amalgamated continental terranes, East Antarctica craton, and the Trans-Antarctic belt (*Harley, 2003*).

(b) Exposed bedrock in Antarctica (based on CGMW Geological Map of the World, 2002). Locations marked on the map are discussed in text. Colors show rock ages.

Fig. 3. Equivalent topography map (for density of ice 0.92 g/cm^3 and of water 1.02 g/cm^3 corrected to density 2.67 g/cm^3). This map forms basis for our new tectonic model of West Antarctica with subduction-related volcanic arc and back-arc basins.

Also shown are: (a) Color-coded numbers - age of volcanism (*Kyle & Muncy, 1989; Collinson et al., 1994; Mukasa & Dalziel, 2000; Harley, 2003*). **(b)** Color dots - seismicity by depth since 1916 from USGS catalogue (<https://earthquake.usgs.gov/earthquakes/search/>). Red triangles - Cenozoic volcanoes. Black lines – paleosubduction system with proposed subduction jump. Labels a-j mark the western end of profiles in **Fig. 8**.

Fig. 4. (a) Crustal thickness in Antarctica compiled from various sources (*Baranov & Morelli, 2013; updated by results from Chaput et al., 2014; Feng et al., 2014; An et al., 2015b; Hansen et al., 2016; Ramirez et al., 2016*). In our compilation, we do not use gravity constraints on crustal thickness (e.g. *Block et al., 2009*). **Symbols** – locations of seismic stations.

(b) Seismic Moho depths (from sea level) grouped into classes by tectonic setting. Average values for each tectonic group are used in correlation analysis (**Fig. 12**).

Fig. 5. Lithosphere thickness in Antarctica (a) based on a seismic tomography model (*An et al., 2015b*), with the LAB defined by a 1% velocity perturbation;

(b) based on thermal TC1 model (*Artemieva, 2006*).

Fig. 6. Hypsometry based on ETOPO1 global model. WA – equivalent hypsometry in West Antarctica (corrected for water and ice) extends down to -1580 m with an average value of $-580 \pm 335 \text{ m}$. In other back-arc basins average values of equivalent hypsometry are between ca. -3000 m and -300 m (**Table 1**).

Fig. 7. Plate reconstructions of the region around West Antarctica (after *Musaka and Dalziel, 2000*) illustrating the Mesozoic subduction of the Phoenix Plate in paleo-reconstructions between 117 and 30 Ma. Location of the subduction trench is emphasized by a purple line and purple arrows illustrate locations of back-arc spreading and extension. Abbreviations: West Antarctica crustal blocks (red): AP - Antarctic Peninsula; EWM - Ellsworth-Whitmore Mountains; MBL - Marie Byrd Land; TI - Thurston Island; Other blocks: AUS - Australia; CHP - Challenger Plateau; CP - Campbell Plateau (east and west); CR—Chatham Rise; LF—Lafonian microplate; LHR—Lord Howe Rise; NZ -

1535
1536
1537 1029 New Zealand (east and west); SAM - South America. Red-arrowed line in 85 Ma
1538 1030 reconstruction is incipient Pacific-Antarctic spreading center between the Marie Byrd
1539 1031 Land crustal block and the New Zealand microcontinent; dark red lines are spreading
1540 1032 ridges.

1541 1033 **Fig. 8.** Topography, seismicity and gravity anomalies across the Pacific margin of West
1542 1034 Antarctica along a series of profiles perpendicular to the paleosubduction trench (see
1543 1035 **Fig. 3b** for locations).

1544 1036 **(a)** Free air anomalies across the central part of the West Antarctica Pacific margin
1545 1037 along three profiles aligned to start at the trench (e - solid line; h - dashed line; I -
1546 1038 dotted line). Similar to other subduction systems, the trench has negative and the
1547 1039 volcanic arc has slightly positive free air anomalies.

1548 1040 **(b)** Equivalent hypsometry (top, lines), volcanoes (top, triangles) and seismicity
1549 1041 (bottom, circles) profiles. Color codes for lines and symbols refer to profiles in **Fig. 3b**.
1550 1042 Data for the Japan subduction and volcanic arc at 40°N are shown for comparison.

1551 1043 **Fig. 9.** Comparison of back-arc basins of the world (see **Fig. 10** for locations and **Table 1** for
1552 1044 details). Color-coded boxes show typical range of values. Black boxes - typical values
1553 1045 for regions of West Antarctica with negative equivalent topography. West Antarctica is
1554 1046 particularly similar to back-arc basins of the Tyrrhenian, Andaman, Okinawa and
1555 1047 Aegean systems.

1556 1048 **Fig. 10.** Location of back-arc basins of the world listed in **Table 1**. The proposed system of
1557 1049 back-arc basins of West Antarctica is mostly outside the map.

1558 1050 **Fig. 11. Gravity anomalies.**

1559 1051 **(a)** Free air anomaly for onshore (*Scheinert et al., 2016*) and offshore (*Pavlis et al.,*
1560 1052 *2012*) area. Gravity anomalies across the Pacific margin of West Antarctica are similar
1561 1053 to active subduction systems with the trench between the two arrows (*Artemieva et al.,*
1562 1054 *2016*). **Dots** - seismicity since 1916 (based on USGS catalogue). **Colored symbols** -
1563 1055 depth to Moho from sea level based on reflection/refraction data (boxes) and seismic
1564 1056 receiver functions (triangles).

1565 1057 **(b)** Bouguer anomaly (reduction density 2.67 g/cm³). Colored symbols - depth to Moho
1566 1058 from sea level based on reflection/refraction data (boxes) and seismic receiver functions
1567 1059 (triangles).

1568 1060 **Fig. 12.** Equivalent topography versus crustal thickness for back-arc basins in the world and
1569 1061 for tectonic provinces in Antarctica. Tectonic locations for Antarctica are shown in **Fig.**
1570 1062 **4b**. Other back-arc basins are described in **Table 1** and shown in **Fig. 10**. Horizontal and
1571 1063 vertical bars: standard deviations for locations in Antarctica and the span of values for
1572 1064 back-arc basins in the world. Star - average values for areas of West Antarctica below
1573 1065 sea level. Best fit lines are based on locations 1b-7 for East Antarctica craton and for
1574 1066 locations 8-13 and back-arc basins in the world for back-arcs. For some back-arc basins
1575 1067 crustal thickness is unknown.

1594
1595
1596 1068 **Fig. 13.** Density contrast between the crust and the upper mantle assuming Airy-type
1597 1069 isostasy. Vertical axis – slope of the equivalent topography versus crustal thickness
1599 1070 trend. Horizontal axes – mantle density at in situ conditions (bottom) and recalculated
1600 1071 to room (SPT) conditions for two different in situ temperatures.

1601
1602 1072 **Fig. 14.** (a) Residual mantle gravity anomalies calculated by subtracting the crustal
1603 1073 contribution based on crustal thickness (Fig. 4a) for constant density of 2.8 g/cm³.
1604 1074 Reference model: 40 km thick crust with density 2.8 g/cm³ above 30 km thick mantle
1605 1075 layer with density 3.35 g/cm³.

1607 1076 (b) Depth to Curie point based on airborne magnetic data (Martos et al., 2017).

1608
1609 1077 **Fig. 15.** Lithosphere density calculated for two end-member scenarios to fit mantle residual
1610 1078 gravity anomaly (Fig. 14a) and seismic data on crustal thickness (Fig. 4).

1611
1612 1079 (a) Crustal density assuming that all mantle residual gravity anomaly is caused solely
1613 1080 by density variations in the crust. The model is calibrated by seismic data at the
1614 1081 reference point in East Antarctica, where crustal density is assumed 2.8 g/cm³.

1615
1616 1082 (b) Lithospheric mantle density at standard P-T conditions (room temperature and
1617 1083 pressure) for the lithospheric layer between the Moho and the seismic LAB (An et al.,
1618 1084 2015a) (Fig. S2b), assuming constant crustal density of 2.8 g/cm³.

1619
1620 1085 **Fig. 16.** New model of the Antarctica continent and the West Antarctica back-arc system
1621 1086 behind the volcanic arc formed by Mesozoic subduction. The possible <S> volcanic arc
1622 1087 is proposed to explain the Wilkes basin within the framework of the “Atlantic” and
1624 1088 “Pacific” back-arc basins, although less constrained by our geophysical data.

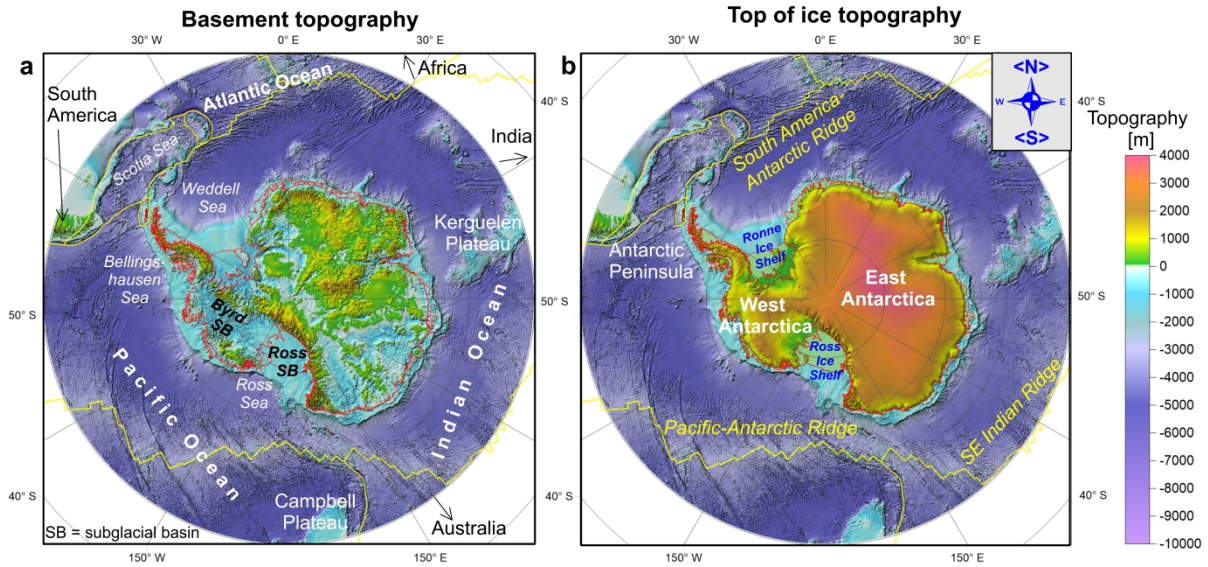
1625 1089

1626 1090

Table 1. Geophysical characteristics of back-arcs of the world

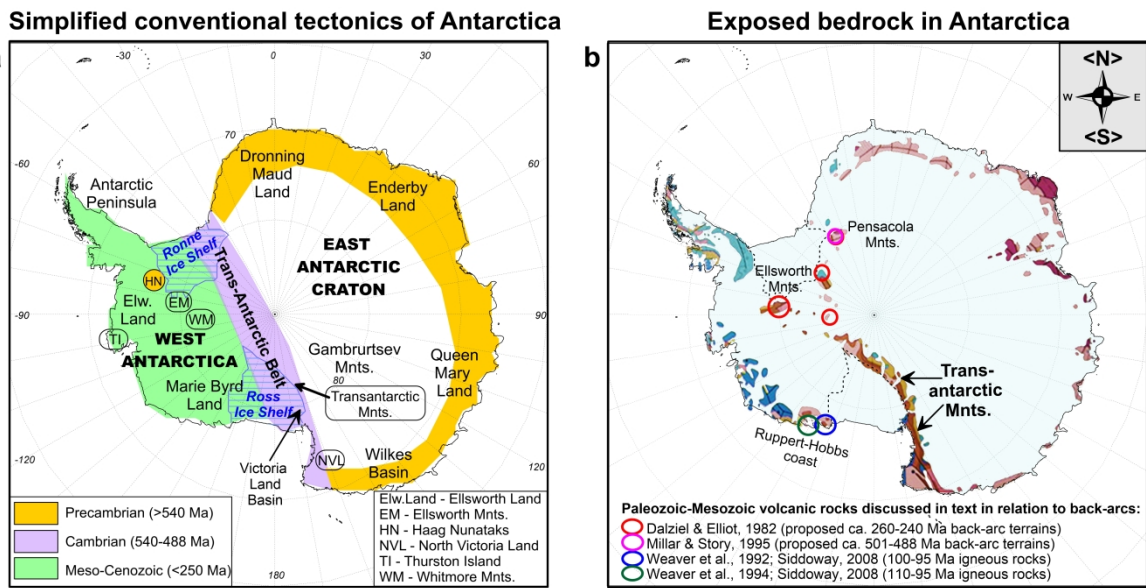
No.	Back-arcs	Bathymetry (m)	Equivalent topography (m)	Free air anomalies (mGal)	Bouguer anomalies (mGal)	Crustal thickness from seismic data (km)
	Active					
2	Tyrrhenian Sea	-3000 to -1000	-1875 to -625	-30 to +20	+20 to +180	Ca. 8 km (<i>Sartori et al., 2004</i>)
3	Andaman Sea	-3000 to -500	-1875 to -310	-20 to +40	0 to +200	N/A
4	Aegean Sea	-1500 to -800	-950 to -500	+30 to +100	+100 to +150	Ca. 25 km (<i>Zhu et al., 2006</i>)
5	Okinawa Trough	-1000 to -100	-625 to -60	0 to +40	+100 to +150	23-27 km (<i>Nakamura & Umedu, 2009</i>)
8	Lau Basin	-2500 to -1700	-1560 to -1060	+10 to +70	+90 to +200	5-10 km (<i>Crawford et al., 2003</i>)
9	Mariana Trough	-4000 to -3000	-2500 to -1875	-30 to +50	+200 to +300	5-7 km (<i>Takahashi et al., 2007</i>)
10	E. Scotia Sea	-4000 to -3000	-2500 to -1875	+10 to +40	+200 to +300	N/A
	Extinct					
6	Sea of Japan	-3000 to -500	-1875 to -310	-15 to +40	+100 to +250	15-20 km (<i>Iwasaki et al., 2003</i>)
7	Kurile Basin	-3000 to -1000	-1875 to -625	-30 to +30	+100 to +250	N/A
11	Banda Basins	-4000 to -1800	-2500 to -1130	+10 to +100	+250 to +350	N/A
12	Parece-Vela	-5000 to -2000	-3125 to -1250	-20 to +40	+250 to +350	N/A
13	Gulf of Mexico	-5000 to -1500	-3125 to -950	-20 to +15	+150 to +320	7-10 km (<i>Christeson et al., 2014</i>)
14	W. Philippine Sea	-5500 to -4500	-3440 to -2810	-5 to +20	+350 to +400	3-5 km (<i>Goodman et al., 1989</i>)
1	West Antarctica (only regions with negative equivalent topography)	-675±350 (-1850 to 0)	-580±335 (-1580 to 0)	-23±20 (-40 to +20)	5±23 (-30 to +50)	25±5.7 km (14 km to 40 km) (<i>Baranov & Morelli, 2013; Feng et al., 2014; An et al., 2015b; Ramirez et al., 2016</i>)

1712
1713
1714
1715 1093 **Figures**
1716
1717
1718



1734 1094 **Fig. 1.** Basement topography (a) and topography of the ice sheet (b) in the Antarctic region.

1735 1095
1736
1737 1096
1738



1757 1097
1758 1098 **Fig. 2. (a)** Classic concept of Antarctica consisting of three domains: West Antarctica made
1759 1099 of several amalgamated continental terranes, East Antarctica craton, and the Trans-
1760 1100 Antarctic belt (*Harley, 2003*).

1761
1762 1101 **(b)** Exposed bedrock in Antarctica (based on CGMW Geological Map of the World,
1763 1102 2002). Locations marked on the map are discussed in text. Colors show rock ages.

1764
1765 1103
1766
1767
1768
1769
1770

1771
1772
1773
1774
1775
1776
1777
1778
1779
1780
1781
1782
1783
1784
1785
1786
1787
1788
1789
1791
1792
1793
1794
1795
1796
1797
1798
1799
1800
1801
1802
1803
1804
1805
1806
1807
1808
1809
1810
1811
1812
1813
1814
1815
1816
1817
1818
1819
1820
1821
1822
1823
1824
1825
1826
1827
1828
1829

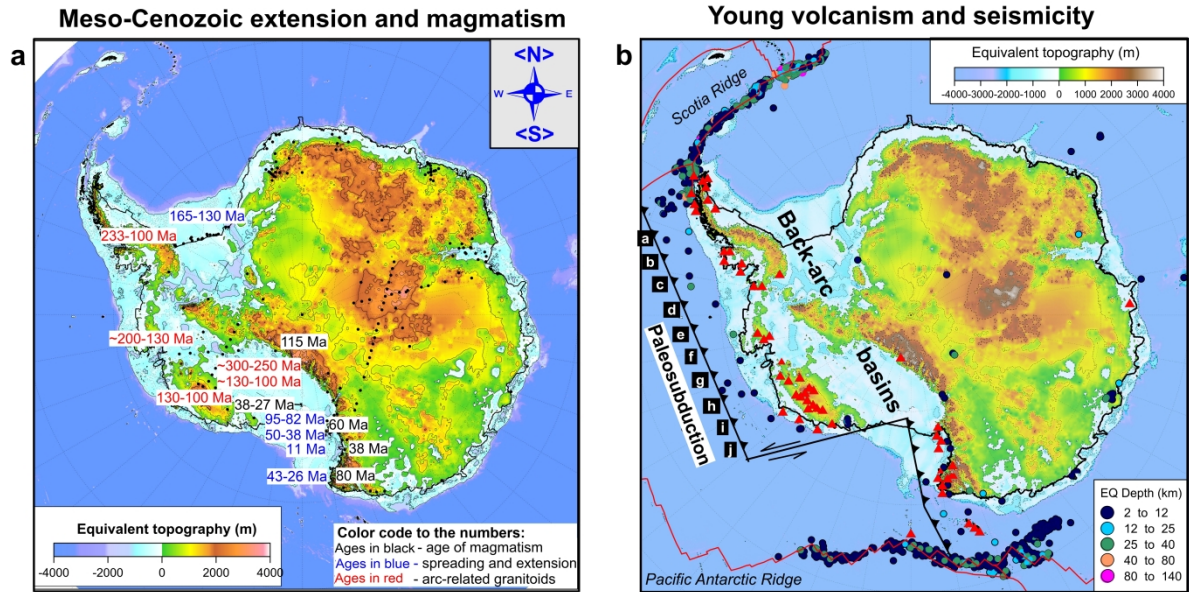


Fig. 3. Equivalent topography map (for density of ice 0.92 g/cm^3 and of water 1.02 g/cm^3 , corrected to density 2.67 g/cm^3). This map forms basis for our new tectonic model of West Antarctica with subduction-related volcanic arc and back-arc basins. **Also shown are:** (a) Color-coded numbers - age of volcanism (*Kyle & Muncy, 1989; Collinson et al., 1994; Mukasa & Dalziel, 2000; Harley, 2003*). (b) Color dots - seismicity by depth since 1916 from USGS catalogue (<https://earthquake.usgs.gov/earthquakes/search/>). Red triangles - Cenozoic volcanoes. Black lines – paleosubduction system with proposed subduction jump. Labels a-j mark the western end of profiles in Fig. 8.

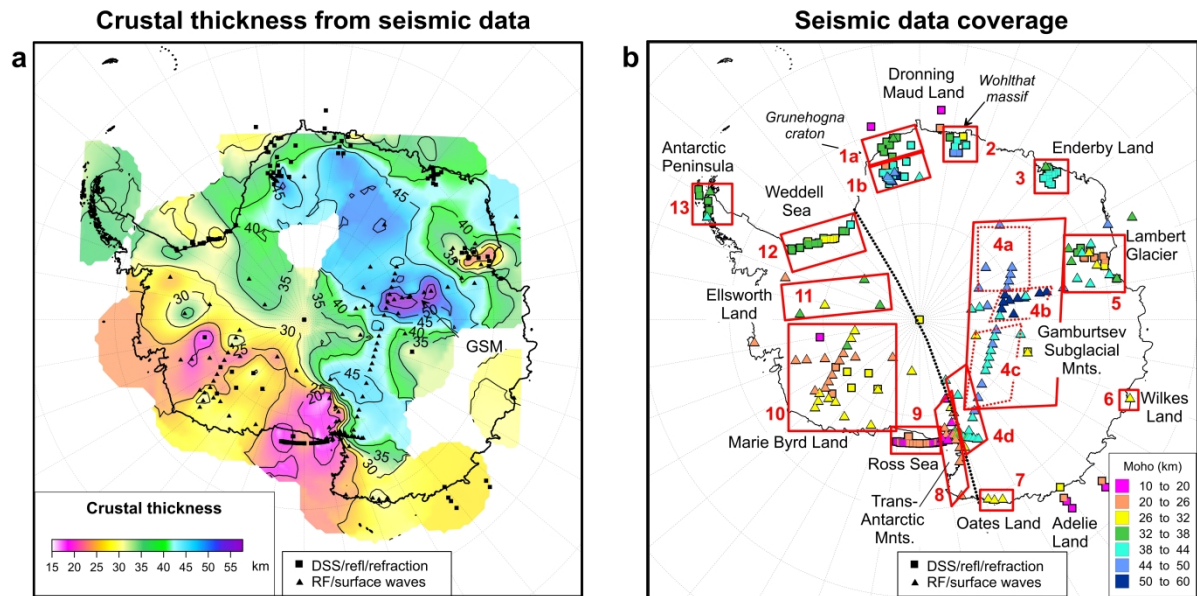


Fig. 4. (a) Crustal thickness in Antarctica compiled from various sources (*Baranov & Morelli, 2013*; updated by results from *Chaput et al., 2014; Feng et al., 2014; An et al., 2015b; Hansen et al., 2016; Ramirez et al., 2016*). In our compilation, we do not use gravity constraints on crustal thickness (e.g. *Bloch et al., 2009*). **Symbols** – locations of seismic stations.

(b) Seismic Moho depths (from sea level) grouped into classes by tectonic setting. Average values for each tectonic group are used in correlation analysis (Fig. 12).

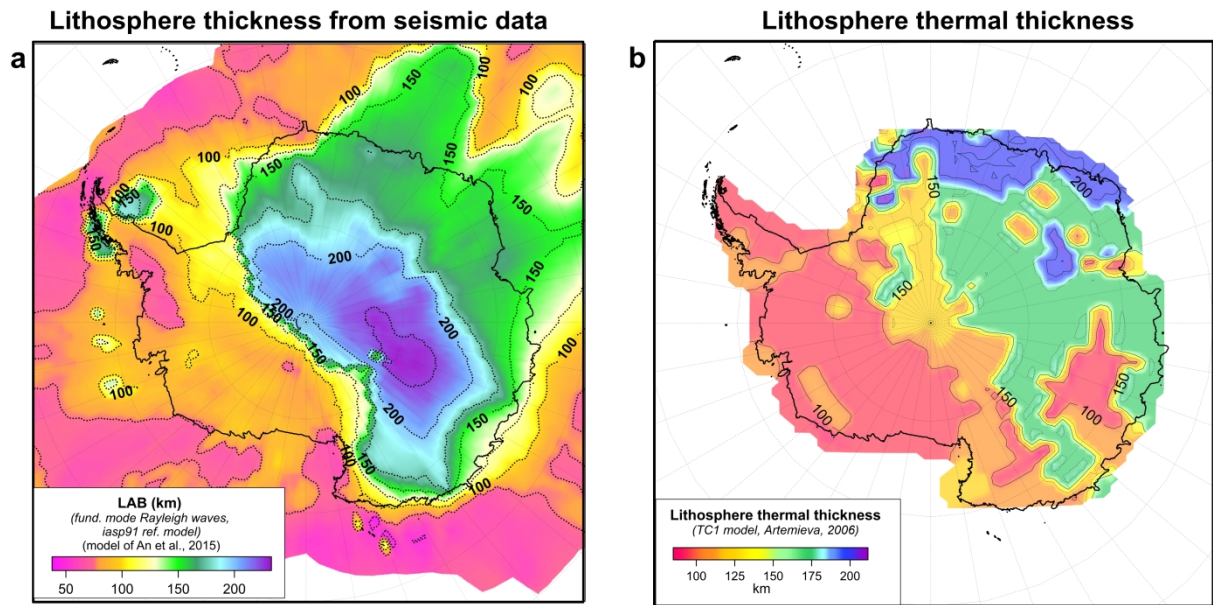
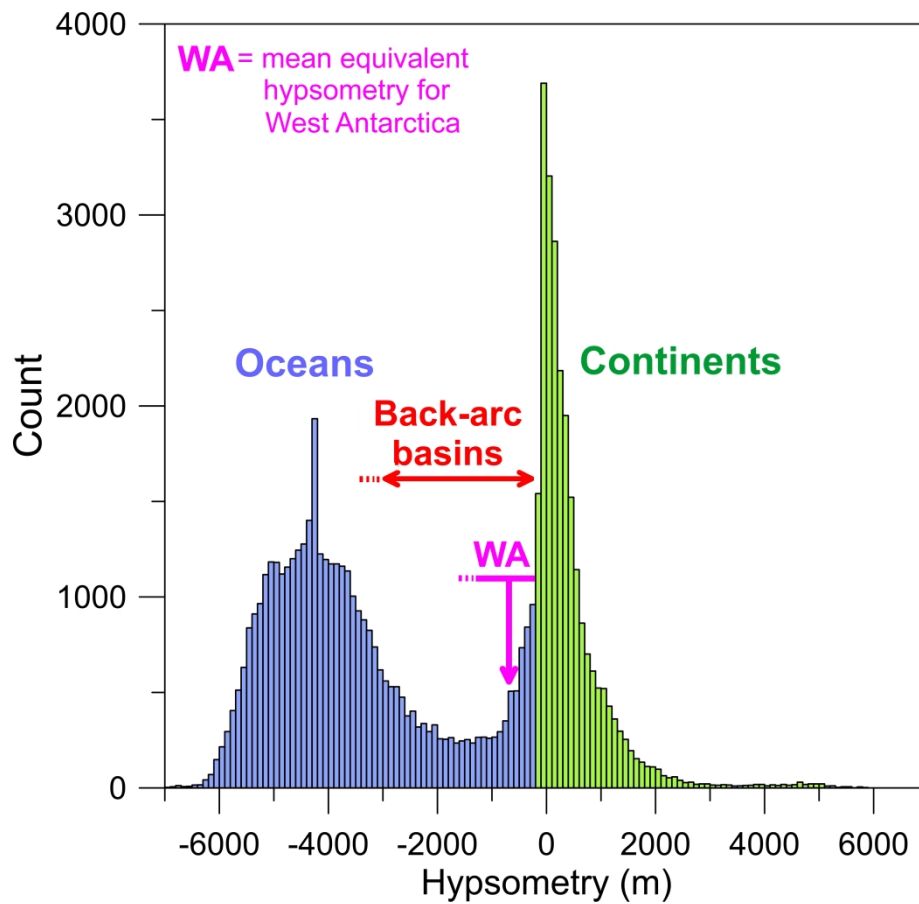


Fig. 5. Lithosphere thickness in Antarctica (a) based on a seismic tomography model (*An et al., 2015b*), with the LAB defined by a 1% velocity perturbation; (b) based on thermal TC1 model (*Artemieva, 2006*).

1124



1125

1126

1127

1128

1129

1130

Fig. 6. Hypsometry based on ETOPO1 global model. WA – equivalent hypsometry in West Antarctica (corrected for water and ice) extends down to -1580 m with an average value of -580 ± 335 m. In other back-arc basins average values of equivalent hypsometry are between ca. -3000 m and -300 m (Table 1).

1927

1928

1929

1930

1931

1932

1933

1934

1935

1936

1937

1938

1939

1940

1941

1942

1943

1944

1945

1946

1947

1948
 1949
 1950
 1951 1131
 1952
 1953
 1954
 1955
 1956
 1957
 1958
 1959
 1960
 1961
 1962
 1963
 1964
 1965
 1966
 1967
 1968 1132
 1969
 1970 1133
 1971 1134
 1972 1135
 1973 1136
 1974 1137
 1975 1138
 1976 1139
 1977 1140
 1978 1141
 1979 1142
 1980 1143
 1981 1144
 1982
 1983
 1984
 1985
 1986
 1987
 1988
 1989
 1990
 1991
 1992
 1993
 1994
 1995
 1996
 1997
 1998
 1999
 2000
 2001
 2002
 2003
 2004
 2005
 2006

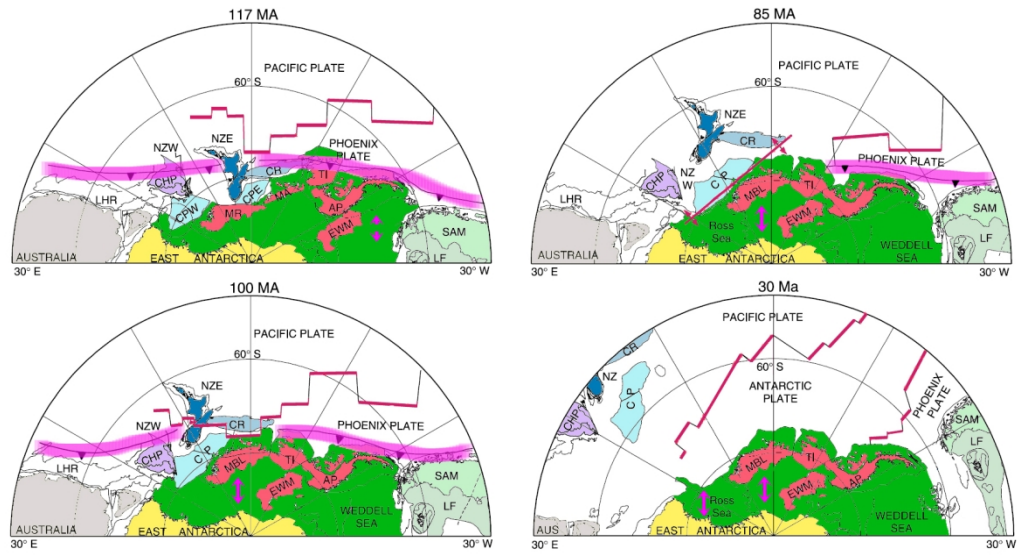


Fig. 7. Plate reconstructions of the region around West Antarctica (after *Musaka and Dalziel, 2000*) illustrating the Mesozoic subduction of the Phoenix Plate in paleoreconstructions between 117 and 30 Ma. Location of the subduction trench is emphasized by a purple line and purple arrows illustrate locations of back-arc spreading and extension. Abbreviations: West Antarctica crustal blocks (red): AP - Antarctic Peninsula; EWM - Ellsworth-Whitmore Mountains; MBL - Marie Byrd Land; TI - Thurston Island; Other blocks: AUS - Australia; CHP - Challenger Plateau; CP - Campbell Plateau (east and west); CR—Chatham Rise; LF—Lafonian microplate; LHR—Lord Howe Rise; NZ - New Zealand (east and west); SAM - South America. Red-arrowed line in 85 Ma reconstruction is incipient Pacific-Antarctic spreading center between the Marie Byrd Land crustal block and the New Zealand microcontinent; dark red lines are spreading ridges.

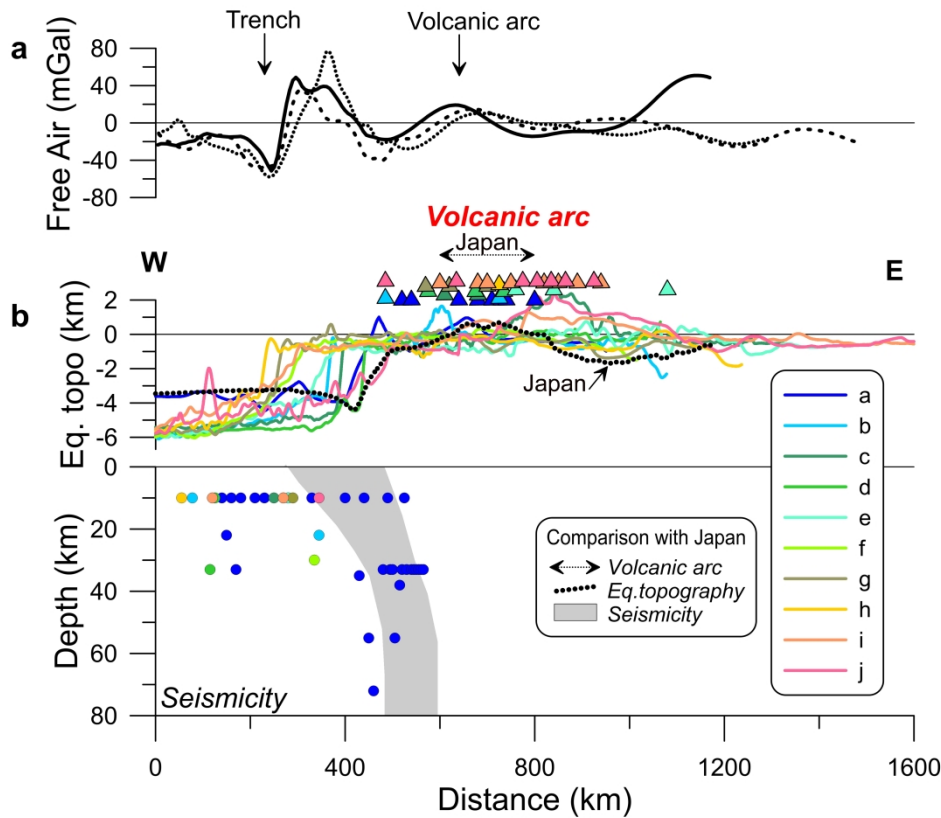


Fig. 8. Topography, seismicity and gravity anomalies across the Pacific margin of West Antarctica along a series of profiles perpendicular to the paleosubduction trench (see Fig. 3b for locations).

(a) Free air anomalies across the central part of the West Antarctica Pacific margin along three profiles aligned to start at the trench (e - solid line; h - dashed line; I - dotted line). Similar to other subduction systems, the trench has negative and the volcanic arc has slightly positive free air anomalies.

(b) Equivalent hypsometry (top, lines), volcanoes (top, triangles) and seismicity (bottom, circles) profiles. Color codes for lines and symbols refer to profiles in Fig. 3b. Data for the Japan subduction and volcanic arc at 40°N are shown for comparison.

2066
 2067
 2068
 2069
 2070
 2071
 2072
 2073
 2074
 2075
 2076
 2077
 2078
 2079
 2080
 2081
 2082
 2083
 2084
 2085
 2086
 2087
 2088
 2089
 2090
 2091
 2092
 2093
 2094
 2095
 2096
 2097
 2098
 2099
 2100
 2101
 2102
 2103
 2104
 2105
 2106
 2107
 2108
 2109
 2110
 2111
 2112
 2113
 2114
 2115
 2116
 2117
 2118
 2119
 2120
 2121
 2122
 2123
 2124

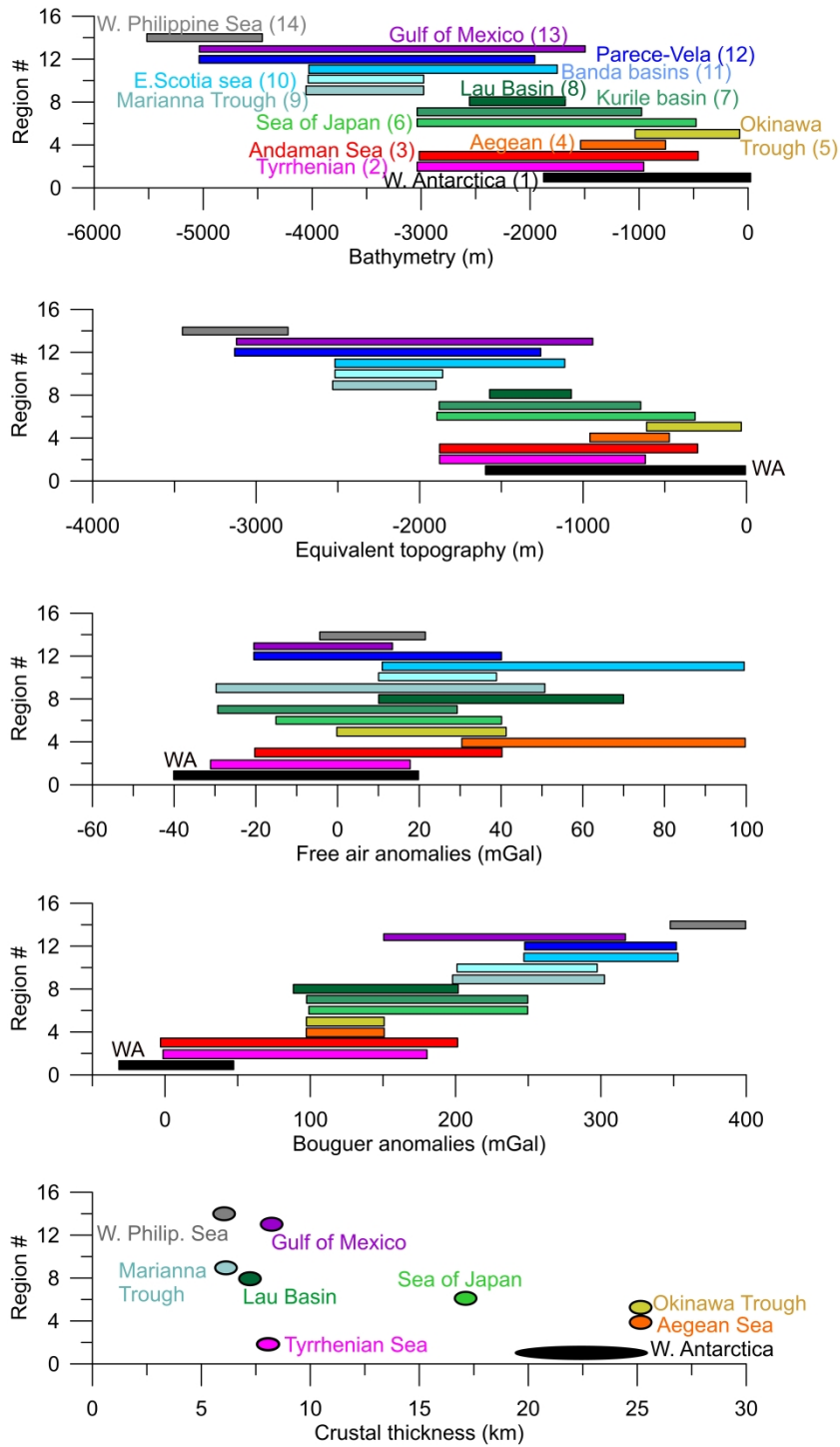


Fig. 9. Comparison of back-arc basins of the world (see Fig. 10 for locations and Table 1 for details). Color-coded boxes show typical range of values. Black boxes – typical values for regions of West Antarctica with negative equivalent topography. West Antarctica is particularly similar to back-arc basins of the Tyrrhenian, Andaman, Okinawa and Aegean systems.

2125
2126
2127
2128
2129
2130
2131
2132
2133
2134
2135
2136
2137
2138
2139
2140
2141
2142
2143
2144
2145
2146
2147
2148
2149
2150
2151
2152
2153
2154
2155
2156
2157
2158
2159
2160
2161
2162
2163
2164
2165
2166
2167
2168
2169
2170
2171
2172
2173
2174
2175
2176
2177
2178
2179
2180
2181
2182
2183

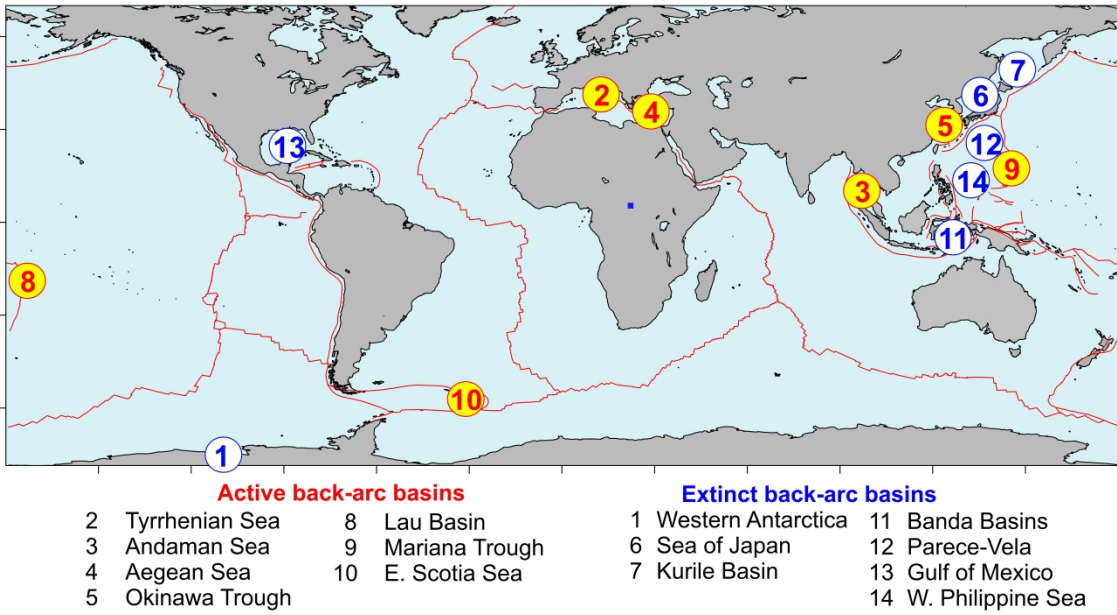


Fig. 10. Location of back-arc basins of the world listed in Table 1. The proposed system of back-arc basins of West Antarctica is mostly outside the map.

2184
 2185
 2186
 1169 2187
 1170 2188
 2189
 2190
 2191
 2192
 2193
 2194
 2195
 2196
 2197
 2198
 2199
 2200
 2201
 2202
 2203
 2204
 2205
 2206
 1171 2207
 1172 2208
 1173 2209
 1174 2210
 1175 2211
 1176 2212
 1177 2213
 1178 2214
 1179 2215
 1180 2216
 1181 2217
 1182 2218
 2219
 2220
 2221
 2222
 2223
 2224
 2225
 2226
 2227
 2228
 2229
 2230
 2231
 2232
 2233
 2234
 2235
 2236
 2237
 2238
 2239
 2240
 2241
 2242

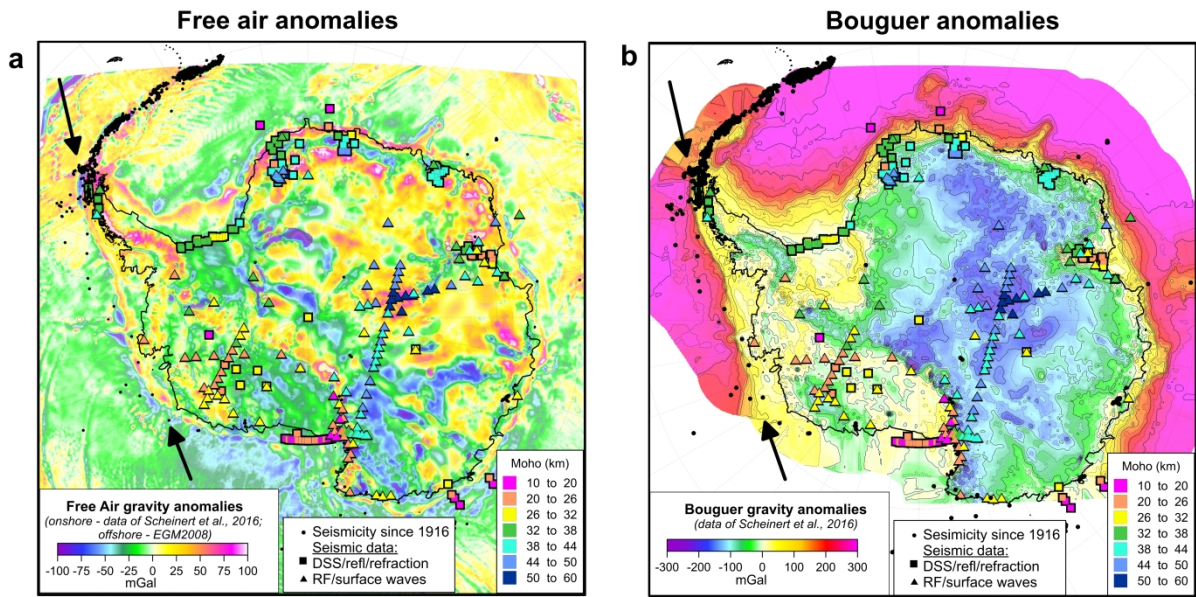
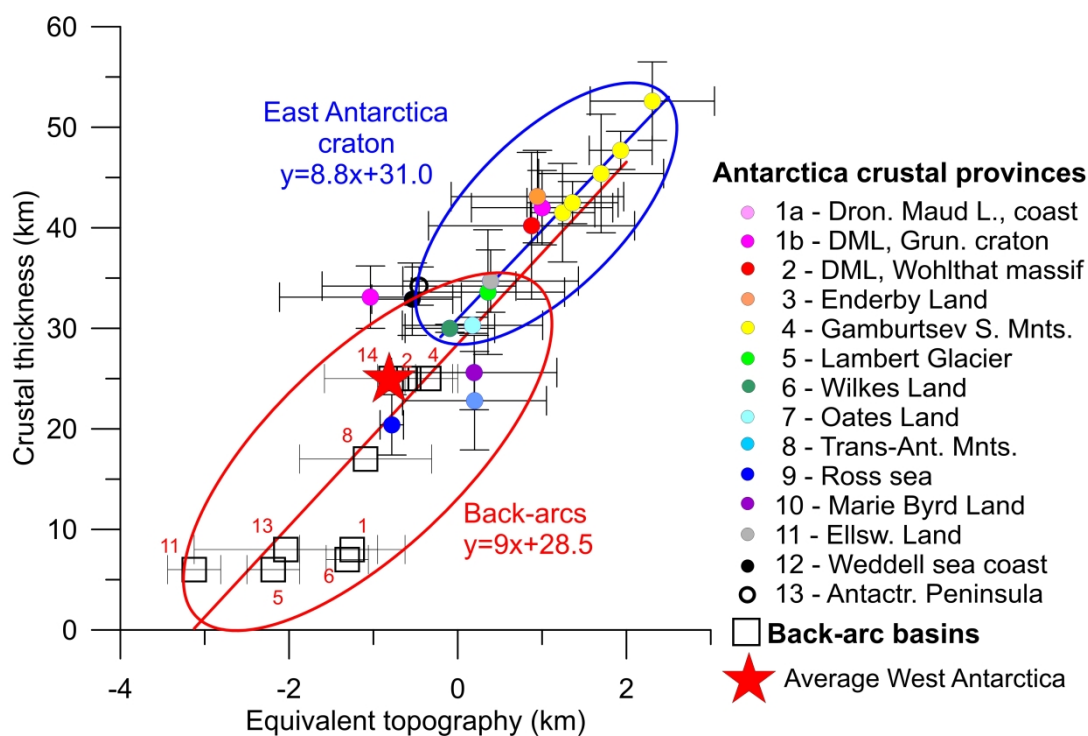


Fig. 11. Gravity anomalies.

(a) Free air anomaly for onshore (Scheinert et al., 2016) and offshore (Pavlis et al., 2012) area. Gravity anomalies across the Pacific margin of West Antarctica are similar to active subduction systems with the trench between the two arrows (Artemieva et al., 2016). **Dots** - seismicity since 1916 (based on USGS catalogue). **Colored symbols** - depth to Moho from sea level based on reflection/refraction data (boxes) and seismic receiver functions (triangles).

(b) Bouguer anomaly (reduction density 2.67 g/cm³). Colored symbols - depth to Moho from sea level based on reflection/refraction data (boxes) and seismic receiver functions (triangles).



2243
2244
2245 1183
2246
2247 1184
2248
2249 1185
2250 1186
2251 1187
2252
2253 1188
2254 1189
2255 1190
2256 1191
2257 1192
2258
2259 1193
2260
2261 1194
2262
2263
2264
2265
2266
2267
2268
2269
2270
2271
2272
2273
2274
2275
2276
2277
2278
2279
2280
2281
2282
2283
2284
2285
2286
2287
2288
2289
2290
2291
2292
2293
2294
2295
2296
2297
2298
2299
2300
2301

Fig. 12. Equivalent topography versus crustal thickness for back-arc basins in the world and for tectonic provinces in Antarctica. Tectonic locations for Antarctica are shown in **Fig. 4b**. Other back-arc basins are described in **Table 1** and shown in **Fig. 10**. Horizontal and vertical bars: standard deviations for locations in Antarctica and the span of values for back-arc basins in the world. Star – average values for areas of West Antarctica below sea level. Best fit lines are based on locations 1b-7 for East Antarctica craton and for locations 8-13 and back-arc basins in the world for back-arcs. For some back-arc basins crustal thickness is unknown.

1195

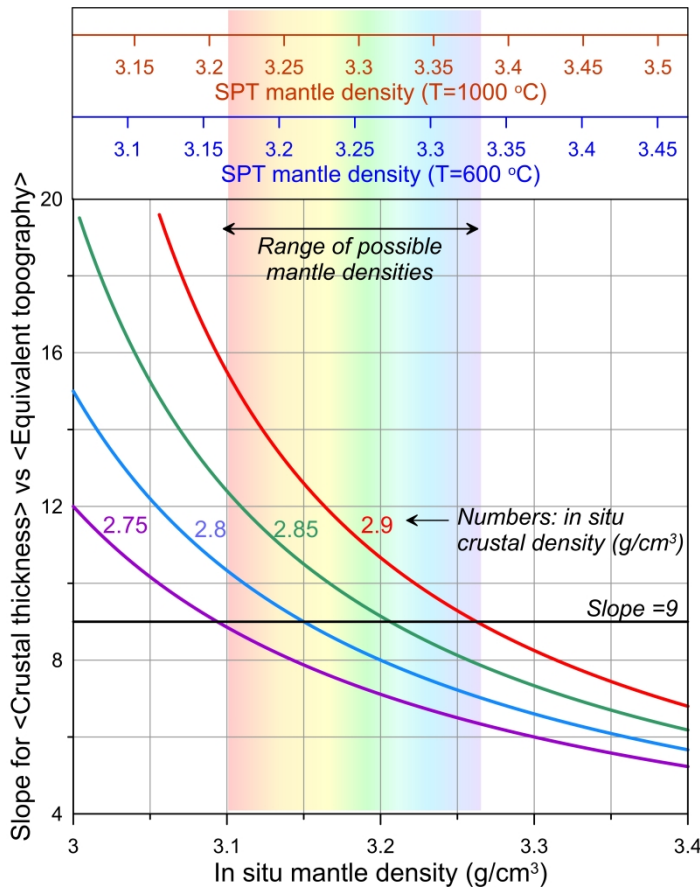


Fig. 13. Density contrast between the crust and the upper mantle assuming Airy-type isostasy. Vertical axis – slope of the equivalent topography versus crustal thickness trend. Horizontal axes – mantle density at in situ conditions (bottom) and recalculated to room (SPT) conditions for two different in situ temperatures.

2361
2362
2363
2364
2365
2366
2367
2368
2369
2370
2371
2372
2373
2374
2375
2376
2377
2378
2379
2380
2381
2382 1202
2383 1203
2384 1204
2385 1205
2386 1206
2387
2388
2389
2390
2391
2392
2393
2394
2395
2396
2397
2398
2399
2400
2401
2402
2403
2404
2405
2406
2407 1207
2408 1208
2409 1209
2410 1210
2411 1211
2412
2413 1212
2414 1213
2415 1214
2416
2417
2418
2419

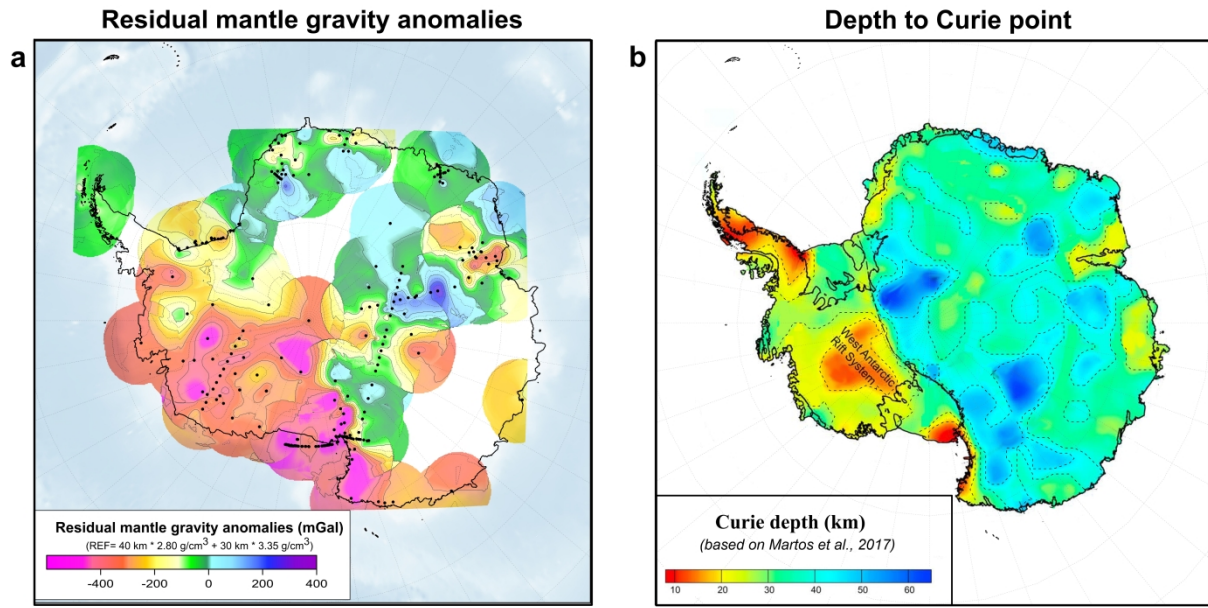


Fig. 14. (a) Residual mantle gravity anomalies calculated by subtracting the crustal contribution based on crustal thickness (Fig. 4a) for constant density of 2.8 g/cm^3 . Reference model: 40 km thick crust with density 2.8 g/cm^3 above 30 km thick mantle layer with density 3.35 g/cm^3 . (b) Depth to Curie point based on airborne magnetic data (Martos et al., 2017).

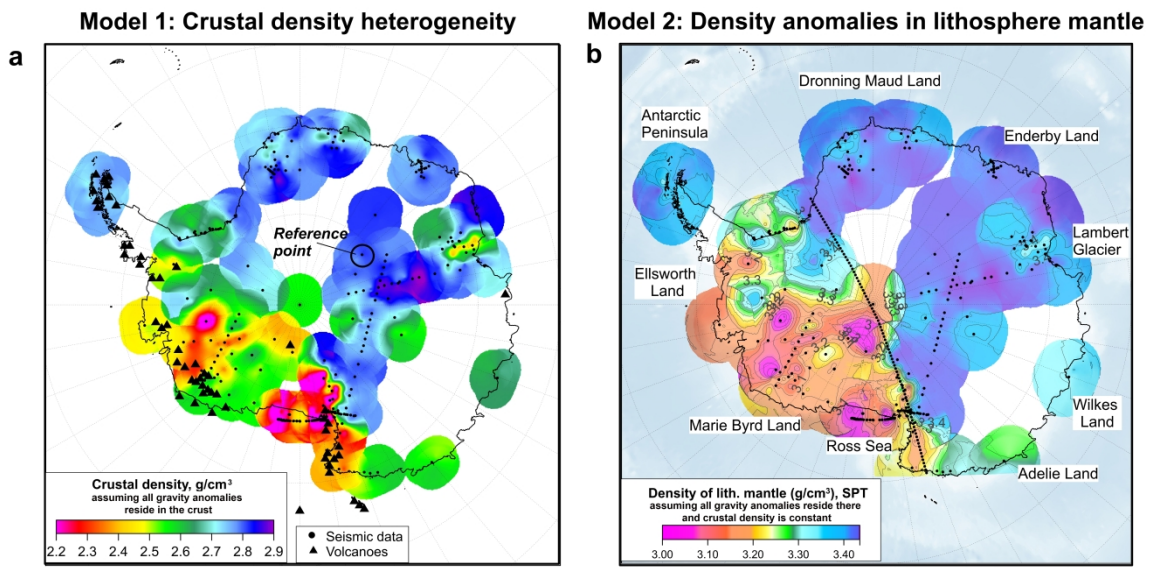
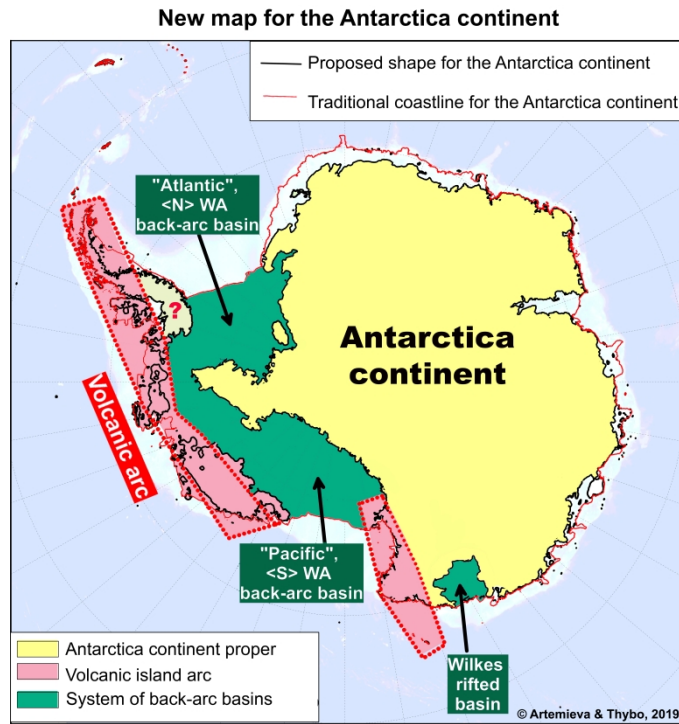


Fig. 15. Lithosphere density calculated for two end-member scenarios to fit mantle residual gravity anomaly (Fig. 14a) and seismic data on crustal thickness (Fig. 4).
(a) Crustal density assuming that all mantle residual gravity anomaly is caused solely by density variations in the crust. The model is calibrated by seismic data at the reference point in East Antarctica, where crustal density is assumed 2.8 g/cm^3 .
(b) Lithospheric mantle density at standard P-T conditions (room temperature and pressure) for the lithospheric layer between the Moho and the seismic LAB (An et al., 2015a) (Fig. S2b), assuming constant crustal density of 2.8 g/cm^3 .

1215



1216

1217

1218

Fig. 16. New model of the Antarctica continent and the West Antarctica back-arc system behind the volcanic arc formed by Mesozoic subduction. The possible <S> volcanic arc is proposed to explain the Wilkes basin within the framework of the “Atlantic” and “Pacific” back-arc basins, although less constrained by our geophysical data.

1220

1221

1222

1223

1224

1225

1226

1227

1228

1229

1230

1231

1232

1233

1234

1235

1236

1237

1238

1 **Table 1. Geophysical characteristics of back-arcs of the world**

No.	Back-arcs	Bathymetry (m)	Equivalent topography (m)	Free air anomalies (mGal)	Bouguer anomalies (mGal)	Crustal thickness from seismic data (km)
	Active					
2	Tyrrhenian Sea	-3000 to -1000	-1875 to -625	-30 to +20	+20 to +180	Ca. 8 km (<i>Sartori et al., 2004</i>)
3	Andaman Sea	-3000 to -500	-1875 to -310	-20 to +40	0 to +200	N/A
4	Aegean Sea	-1500 to -800	-950 to -500	+30 to +100	+100 to +150	Ca. 25 km (<i>Zhu et al., 2006</i>)
5	Okinawa Trough	-1000 to -100	-625 to -60	0 to +40	+100 to +150	23-27 km (<i>Nakamura & Umedu, 2009</i>)
8	Lau Basin	-2500 to -1700	-1560 to -1060	+10 to +70	+90 to +200	5-10 km (<i>Crawford et al., 2003</i>)
9	Mariana Trough	-4000 to -3000	-2500 to -1875	-30 to +50	+200 to +300	5-7 km (<i>Takahashi et al., 2007</i>)
10	E. Scotia Sea	-4000 to -3000	-2500 to -1875	+10 to +40	+200 to +300	N/A
	Extinct					
6	Sea of Japan	-3000 to -500	-1875 to -310	-15 to +40	+100 to +250	15-20 km (<i>Iwasaki et al., 2003</i>)
7	Kurile Basin	-3000 to -1000	-1875 to -625	-30 to +30	+100 to +250	N/A
11	Banda Basins	-4000 to -1800	-2500 to -1130	+10 to +100	+250 to +350	N/A
12	Parece-Vela	-5000 to -2000	-3125 to -1250	-20 to +40	+250 to +350	N/A
13	Gulf of Mexico	-5000 to -1500	-3125 to -950	-20 to +15	+150 to +320	7-10 km (<i>Christeson et al., 2014</i>)
14	W. Philippine Sea	-5500 to -4500	-3440 to -2810	-5 to +20	+350 to +400	3-5 km (<i>Goodman et al., 1989</i>)
1	West Antarctica (only regions with negative equivalent topography)	-675±350 (-1850 to 0)	-580±335 (-1580 to 0)	-23±20 (-40 to +20)	5±23 (-30 to +50)	25±5.7 km (14 km to 40 km) (<i>Baranov & Morelli, 2013; Feng et al., 2014; An et al., 2015b; Ramirez et al., 2016</i>)

2

3

The authors declare no conflict of interest

Irina Artemieva

Hans Thybo